Precision Theory for Heavy Flavour Physics

Mikołaj Misiak
University of Warsaw

"Polish Particle and Nuclear Theory Summit",
Institute of Nuclear Physics, Polish Academy of Sciences, Cracow, November 22nd-24th, 2023

1. **Introduction**
2. **$b \to s\ell^+\ell^-$ transitions and $R_{D^{(*)}}$**
3. **Update on $B_{s(d)} \to \mu^+\mu^-$**
4. **$\mathcal{B}(B \to X_s\gamma)$ – perturbative and non-perturbative contributions**
5. **Precision determinations of V_{cb} from inclusive $B \to X\ell\bar{\nu}$**
6. **Summary**

In new physics models where all the BSM particles have masses $m_1 \equiv \Lambda \leq m_2 \leq m_3 \ldots m_n$, with $\Lambda \gg m_t$, and interact in a perturbative manner, the Standard Model Effective Field Theory (SMEFT) is a useful tool for describing physics phenomena at energy scales well below Λ.

In new physics models where all the BSM particles have masses $m_1 \equiv \Lambda \leq m_2 \leq m_3 \ldots m_n$, with $\Lambda \gg m_t$, and interact in a perturbative manner, the Standard Model Effective Field Theory (SMEFT) is a useful tool for describing physics phenomena at energy scales well below Λ.

$$\mathcal{L}_{\mathrm{SMEFT}} = \mathcal{L}_{\mathrm{SM}} + \frac{1}{\Lambda}\sum_k C_k^{(5)}(\mu) Q_k^{(5)} + \frac{1}{\Lambda^2}\sum_k C_k^{(6)}(\mu) Q_k^{(6)} + \mathcal{O}\left(\frac{1}{\Lambda^3}\right).$$

In new physics models where all the BSM particles have masses $m_1 \equiv \Lambda \leq m_2 \leq m_3 \ldots m_n$, with $\Lambda \gg m_t$, and interact in a perturbative manner, the Standard Model Effective Field Theory (SMEFT) is a useful tool for describing physics phenomena at energy scales well below Λ.

$$\mathcal{L}_{\rm SMEFT} = \mathcal{L}_{\rm SM} + \frac{1}{\Lambda}\sum_k C_k^{(5)}(\mu) Q_k^{(5)} + \frac{1}{\Lambda^2}\sum_k C_k^{(6)}(\mu) Q_k^{(6)} + \mathcal{O}\left(\frac{1}{\Lambda^3}\right).$$

Flavor-changing processes that take place well below the electroweak scale are conveniently described in the Low-energy Effective Field Theory (LEFT) framework.

In new physics models where all the BSM particles have masses $m_1 \equiv \Lambda \leq m_2 \leq m_3 \ldots m_n$, with $\Lambda \gg m_t$, and interact in a perturbative manner, the Standard Model Effective Field Theory (SMEFT) is a useful tool for describing physics phenomena at energy scales well below Λ.

$$\mathcal{L}_{\mathrm{SMEFT}} = \mathcal{L}_{\mathrm{SM}} + \frac{1}{\Lambda}\sum_k C_k^{(5)}(\mu) Q_k^{(5)} + \frac{1}{\Lambda^2}\sum_k C_k^{(6)}(\mu) Q_k^{(6)} + \mathcal{O}\left(\frac{1}{\Lambda^3}\right).$$

Flavor-changing processes that take place well below the electroweak scale are conveniently described in the Low-energy Effective Field Theory (LEFT) framework. LEFT is obtained from SMEFT through decoupling of the W-boson and all the heavier SM particles.

In new physics models where all the BSM particles have masses $m_1 \equiv \Lambda \leq m_2 \leq m_3 \ldots m_n$, with $\Lambda \gg m_t$, and interact in a perturbative manner, the Standard Model Effective Field Theory (SMEFT) is a useful tool for describing physics phenomena at energy scales well below Λ.

$$\mathcal{L}_{\mathrm{SMEFT}} = \mathcal{L}_{\mathrm{SM}} + \frac{1}{\Lambda}\sum_k C_k^{(5)}(\mu) Q_k^{(5)} + \frac{1}{\Lambda^2}\sum_k C_k^{(6)}(\mu) Q_k^{(6)} + \mathcal{O}\left(\frac{1}{\Lambda^3}\right).$$

Flavor-changing processes that take place well below the electroweak scale are conveniently described in the Low-energy Effective Field Theory (LEFT) framework. LEFT is obtained from SMEFT through decoupling of the W-boson and all the heavier SM particles.

$$\begin{aligned}\mathcal{L}_{\mathrm{LEFT}} &= \mathcal{L}_{\mathrm{QCD}\times\mathrm{QED}}(u,d,s,c,b,e,\mu,\tau) + \mathcal{L}_{\mathrm{kin}}(\nu_e,\nu_\mu,\nu_\tau) \\ &\quad + \frac{1}{M_W}\sum_k C_k^{(5)}(\mu) Q_k^{(5)} + \frac{1}{M_W^2}\sum_k C_k^{(6)}(\mu) Q_k^{(6)} + \mathcal{O}\left(\frac{1}{M_W^3}\right).\end{aligned}$$

In new physics models where all the BSM particles have masses $m_1 \equiv \Lambda \leq m_2 \leq m_3 \ldots m_n$, with $\Lambda \gg m_t$, and interact in a perturbative manner, the Standard Model Effective Field Theory (SMEFT) is a useful tool for describing physics phenomena at energy scales well below Λ.

$$\mathcal{L}_{\text{SMEFT}} = \mathcal{L}_{\text{SM}} + \frac{1}{\Lambda}\sum_k C_k^{(5)}(\mu) Q_k^{(5)} + \frac{1}{\Lambda^2}\sum_k C_k^{(6)}(\mu) Q_k^{(6)} + \mathcal{O}\left(\frac{1}{\Lambda^3}\right).$$

Flavor-changing processes that take place well below the electroweak scale are conveniently described in the Low-energy Effective Field Theory (LEFT) framework. LEFT is obtained from SMEFT through decoupling of the W-boson and all the heavier SM particles.

$$\begin{aligned}\mathcal{L}_{\text{LEFT}} &= \mathcal{L}_{\text{QCD}\times\text{QED}}(u,d,s,c,b,e,\mu,\tau) + \mathcal{L}_{\text{kin}}(\nu_e,\nu_\mu,\nu_\tau)\\ &\quad + \frac{1}{M_W}\sum_k C_k^{(5)}(\mu) Q_k^{(5)} + \frac{1}{M_W^2}\sum_k C_k^{(6)}(\mu) Q_k^{(6)} + \mathcal{O}\left(\frac{1}{M_W^3}\right).\end{aligned}$$

Generically: (Measured observable) = (SM contribution) + (BSM effect).

In new physics models where all the BSM particles have masses $m_1 \equiv \Lambda \leq m_2 \leq m_3 \ldots m_n$, with $\Lambda \gg m_t$, and interact in a perturbative manner, the Standard Model Effective Field Theory (SMEFT) is a useful tool for describing physics phenomena at energy scales well below Λ.

$$\mathcal{L}_{\rm SMEFT} = \mathcal{L}_{\rm SM} + \frac{1}{\Lambda}\sum_k C_k^{(5)}(\mu)Q_k^{(5)} + \frac{1}{\Lambda^2}\sum_k C_k^{(6)}(\mu)Q_k^{(6)} + \mathcal{O}\left(\frac{1}{\Lambda^3}\right).$$

Flavor-changing processes that take place well below the electroweak scale are conveniently described in the Low-energy Effective Field Theory (LEFT) framework. LEFT is obtained from SMEFT through decoupling of the W-boson and all the heavier SM particles.

$$\begin{aligned}\mathcal{L}_{\rm LEFT} &= \mathcal{L}_{\rm QCD\times QED}(u,d,s,c,b,e,\mu,\tau) + \mathcal{L}_{\rm kin}(\nu_e,\nu_\mu,\nu_\tau)\\ &\quad + \frac{1}{M_W}\sum_k C_k^{(5)}(\mu)Q_k^{(5)} + \frac{1}{M_W^2}\sum_k C_k^{(6)}(\mu)Q_k^{(6)} + \mathcal{O}\left(\frac{1}{M_W^3}\right).\end{aligned}$$

Generically: $\quad$ (Measured observable) $=$ $\underbrace{\text{(SM contribution)}}_{\text{dominant}}$ $+$ (BSM effect).

In new physics models where all the BSM particles have masses $m_1 \equiv \Lambda \leq m_2 \leq m_3 \dots m_n$, with $\Lambda \gg m_t$, and interact in a perturbative manner, the Standard Model Effective Field Theory (SMEFT) is a useful tool for describing physics phenomena at energy scales well below Λ.

$$\mathcal{L}_{\text{SMEFT}} = \mathcal{L}_{\text{SM}} + \frac{1}{\Lambda}\sum_k C_k^{(5)}(\mu)Q_k^{(5)} + \frac{1}{\Lambda^2}\sum_k C_k^{(6)}(\mu)Q_k^{(6)} + \mathcal{O}\left(\frac{1}{\Lambda^3}\right).$$

Flavor-changing processes that take place well below the electroweak scale are conveniently described in the Low-energy Effective Field Theory (LEFT) framework. LEFT is obtained from SMEFT through decoupling of the W-boson and all the heavier SM particles.

$$\begin{aligned}\mathcal{L}_{\text{LEFT}} &= \mathcal{L}_{\text{QCD}\times\text{QED}}(u,d,s,c,b,e,\mu,\tau) + \mathcal{L}_{\text{kin}}(\nu_e,\nu_\mu,\nu_\tau)\\ &\quad + \frac{1}{M_W}\sum_k C_k^{(5)}(\mu)Q_k^{(5)} + \frac{1}{M_W^2}\sum_k C_k^{(6)}(\mu)Q_k^{(6)} + \mathcal{O}\left(\frac{1}{M_W^3}\right).\end{aligned}$$

Generically: $\quad \text{(Measured observable)} = \underbrace{\text{(SM contribution)}}_{\text{dominant}} + \underbrace{\text{(BSM effect)}}_{\text{subdominant}}.$

In new physics models where all the BSM particles have masses $m_1 \equiv \Lambda \leq m_2 \leq m_3 \ldots m_n$, with $\Lambda \gg m_t$, and interact in a perturbative manner, the Standard Model Effective Field Theory (SMEFT) is a useful tool for describing physics phenomena at energy scales well below Λ.

$$\mathcal{L}_{\rm SMEFT} \;=\; \mathcal{L}_{\rm SM} \;+\; \tfrac{1}{\Lambda}\textstyle\sum_k C_k^{(5)}(\mu) Q_k^{(5)} \;+\; \tfrac{1}{\Lambda^2}\textstyle\sum_k C_k^{(6)}(\mu) Q_k^{(6)} \;+\; \mathcal{O}\left(\tfrac{1}{\Lambda^3}\right).$$

Flavor-changing processes that take place well below the electroweak scale are conveniently described in the Low-energy Effective Field Theory (LEFT) framework. LEFT is obtained from SMEFT through decoupling of the W-boson and all the heavier SM particles.

$$\begin{aligned}\mathcal{L}_{\rm LEFT} \;=\; & \mathcal{L}_{\rm QCD\times QED}(u,d,s,c,b,e,\mu,\tau) \;+\; \mathcal{L}_{\rm kin}(\nu_e,\nu_\mu,\nu_\tau) \\ & +\; \tfrac{1}{M_W}\textstyle\sum_k C_k^{(5)}(\mu) Q_k^{(5)} \;+\; \tfrac{1}{M_W^2}\textstyle\sum_k C_k^{(6)}(\mu) Q_k^{(6)} \;+\; \mathcal{O}\left(\tfrac{1}{M_W^3}\right).\end{aligned}$$

Generically: $\quad$ (Measured observable) $= \underbrace{\text{(SM contribution)}}_{\text{dominant}} + \underbrace{\text{(BSM effect)}}_{\text{subdominant}}.$

$\Rightarrow$ **TH precision necessary**

In new physics models where all the BSM particles have masses $m_1 \equiv \Lambda \leq m_2 \leq m_3 \ldots m_n$, with $\Lambda \gg m_t$, and interact in a perturbative manner, the Standard Model Effective Field Theory (SMEFT) is a useful tool for describing physics phenomena at energy scales well below Λ.

$$\mathcal{L}_{\rm SMEFT} \;=\; \mathcal{L}_{\rm SM} \;+\; \tfrac{1}{\Lambda}\sum_k C_k^{(5)}(\mu) Q_k^{(5)} \;+\; \tfrac{1}{\Lambda^2}\sum_k C_k^{(6)}(\mu) Q_k^{(6)} \;+\; \mathcal{O}\left(\tfrac{1}{\Lambda^3}\right).$$

Flavor-changing processes that take place well below the electroweak scale are conveniently described in the Low-energy Effective Field Theory (LEFT) framework. LEFT is obtained from SMEFT through decoupling of the W-boson and all the heavier SM particles.

$$\begin{aligned}\mathcal{L}_{\rm LEFT} \;=\; & \mathcal{L}_{\rm QCD\times QED}(u,d,s,c,b,e,\mu,\tau) \;+\; \mathcal{L}_{\rm kin}(\nu_e,\nu_\mu,\nu_\tau) \\ & + \tfrac{1}{M_W}\sum_k C_k^{(5)}(\mu) Q_k^{(5)} \;+\; \tfrac{1}{M_W^2}\sum_k C_k^{(6)}(\mu) Q_k^{(6)} \;+\; \mathcal{O}\left(\tfrac{1}{M_W^3}\right).\end{aligned}$$

Generically: $\quad$ (Measured observable) $\;=\; \underbrace{\text{(SM contribution)}}_{\text{dominant}} \;+\; \underbrace{\text{(BSM effect)}}_{\text{subdominant}}.$

$\Rightarrow$ TH precision necessary $\qquad$ rough calculations sufficient

In new physics models where all the BSM particles have masses $m_1 \equiv \Lambda \leq m_2 \leq m_3 \ldots m_n$, with $\Lambda \gg m_t$, and interact in a perturbative manner, the Standard Model Effective Field Theory (SMEFT) is a useful tool for describing physics phenomena at energy scales well below Λ.

$$\mathcal{L}_{\rm SMEFT} = \mathcal{L}_{\rm SM} + \frac{1}{\Lambda}\sum_k C_k^{(5)}(\mu) Q_k^{(5)} + \frac{1}{\Lambda^2}\sum_k C_k^{(6)}(\mu) Q_k^{(6)} + \mathcal{O}\left(\frac{1}{\Lambda^3}\right).$$

Flavor-changing processes that take place well below the electroweak scale are conveniently described in the Low-energy Effective Field Theory (LEFT) framework. LEFT is obtained from SMEFT through decoupling of the W-boson and all the heavier SM particles.

$$\mathcal{L}_{\rm LEFT} = \mathcal{L}_{\rm QCD\times QED}(u,d,s,c,b,e,\mu,\tau) + \mathcal{L}_{\rm kin}(\nu_e,\nu_\mu,\nu_\tau) + \frac{1}{M_W}\sum_k C_k^{(5)}(\mu) Q_k^{(5)} + \frac{1}{M_W^2}\sum_k C_k^{(6)}(\mu) Q_k^{(6)} + \mathcal{O}\left(\frac{1}{M_W^3}\right).$$

Generically: (Measured observable) = $\underbrace{\text{(SM contribution)}}_{\text{dominant}}$ + $\underbrace{\text{(BSM effect)}}_{\text{subdominant}}$.

$\Rightarrow$ TH precision necessary — rough calculations sufficient

Exceptions: neutrino masses, dark matter, ...

In new physics models where all the BSM particles have masses $m_1 \equiv \Lambda \leq m_2 \leq m_3 \ldots m_n$, with $\Lambda \gg m_t$, and interact in a perturbative manner, the Standard Model Effective Field Theory (SMEFT) is a useful tool for describing physics phenomena at energy scales well below Λ.

$$\mathcal{L}_{\rm SMEFT} = \mathcal{L}_{\rm SM} + \tfrac{1}{\Lambda} \textstyle\sum_k C_k^{(5)}(\mu) Q_k^{(5)} + \tfrac{1}{\Lambda^2} \textstyle\sum_k C_k^{(6)}(\mu) Q_k^{(6)} + \mathcal{O}\left(\tfrac{1}{\Lambda^3}\right).$$

Flavor-changing processes that take place well below the electroweak scale are conveniently described in the Low-energy Effective Field Theory (LEFT) framework. LEFT is obtained from SMEFT through decoupling of the W-boson and all the heavier SM particles.

$$\begin{aligned}\mathcal{L}_{\rm LEFT} &= \mathcal{L}_{\rm QCD\times QED}(u,d,s,c,b,e,\mu,\tau) + \mathcal{L}_{\rm kin}(\nu_e,\nu_\mu,\nu_\tau) \\ &\quad + \tfrac{1}{M_W} \textstyle\sum_k C_k^{(5)}(\mu) Q_k^{(5)} + \tfrac{1}{M_W^2} \textstyle\sum_k C_k^{(6)}(\mu) Q_k^{(6)} + \mathcal{O}\left(\tfrac{1}{M_W^3}\right).\end{aligned}$$

Generically: $\quad$ (Measured observable) $= \underbrace{\text{(SM contribution)}}_{\text{dominant}} + \underbrace{\text{(BSM effect)}}_{\text{subdominant}}$.

$\Rightarrow$ TH precision necessary $\qquad$ rough calculations sufficient

Exceptions: neutrino masses, dark matter, ...

In collider physics?

In new physics models where all the BSM particles have masses $m_1 \equiv \Lambda \leq m_2 \leq m_3 \ldots m_n$, with $\Lambda \gg m_t$, and interact in a perturbative manner, the Standard Model Effective Field Theory (SMEFT) is a useful tool for describing physics phenomena at energy scales well below Λ.

$$\mathcal{L}_{\rm SMEFT} = \mathcal{L}_{\rm SM} + \frac{1}{\Lambda}\sum_k C_k^{(5)}(\mu)Q_k^{(5)} + \frac{1}{\Lambda^2}\sum_k C_k^{(6)}(\mu)Q_k^{(6)} + \mathcal{O}\left(\frac{1}{\Lambda^3}\right).$$

Flavor-changing processes that take place well below the electroweak scale are conveniently described in the Low-energy Effective Field Theory (LEFT) framework. LEFT is obtained from SMEFT through decoupling of the W-boson and all the heavier SM particles.

$$\begin{aligned}\mathcal{L}_{\rm LEFT} &= \mathcal{L}_{\rm QCD\times QED}(u,d,s,c,b,e,\mu,\tau) + \mathcal{L}_{\rm kin}(\nu_e,\nu_\mu,\nu_\tau) \\ &+ \frac{1}{M_W}\sum_k C_k^{(5)}(\mu)Q_k^{(5)} + \frac{1}{M_W^2}\sum_k C_k^{(6)}(\mu)Q_k^{(6)} + \mathcal{O}\left(\frac{1}{M_W^3}\right).\end{aligned}$$

Generically: $\quad$ (Measured observable) $= \underbrace{\text{(SM contribution)}}_{\text{dominant}} + \underbrace{\text{(BSM effect)}}_{\text{subdominant}}.$

$\Rightarrow$ TH precision necessary $\qquad$ rough calculations sufficient

Exceptions: neutrino masses, dark matter, ...

In collider physics? $\quad b \to s\ell^+\ell^-$?

In new physics models where all the BSM particles have masses $m_1 \equiv \Lambda \leq m_2 \leq m_3 \ldots m_n$, with $\Lambda \gg m_t$, and interact in a perturbative manner, the Standard Model Effective Field Theory (SMEFT) is a useful tool for describing physics phenomena at energy scales well below Λ.

$$\mathcal{L}_{\rm SMEFT} \;=\; \mathcal{L}_{\rm SM} \;+\; \tfrac{1}{\Lambda}\sum_k C_k^{(5)}(\mu) Q_k^{(5)} \;+\; \tfrac{1}{\Lambda^2}\sum_k C_k^{(6)}(\mu) Q_k^{(6)} \;+\; \mathcal{O}\left(\tfrac{1}{\Lambda^3}\right).$$

Flavor-changing processes that take place well below the electroweak scale are conveniently described in the Low-energy Effective Field Theory (LEFT) framework. LEFT is obtained from SMEFT through decoupling of the W-boson and all the heavier SM particles.

$$\begin{aligned}\mathcal{L}_{\rm LEFT} \;&=\; \mathcal{L}_{\rm QCD\times QED}(u,d,s,c,b,e,\mu,\tau) \;+\; \mathcal{L}_{\rm kin}(\nu_e,\nu_\mu,\nu_\tau)\\ &+\; \tfrac{1}{M_W}\sum_k C_k^{(5)}(\mu) Q_k^{(5)} \;+\; \tfrac{1}{M_W^2}\sum_k C_k^{(6)}(\mu) Q_k^{(6)} \;+\; \mathcal{O}\left(\tfrac{1}{M_W^3}\right).\end{aligned}$$

Generically: (Measured observable) $=$ $\underbrace{\text{(SM contribution)}}_{\text{dominant}}$ $+$ $\underbrace{\text{(BSM effect)}}_{\text{subdominant}}$.

$\Rightarrow$ TH precision necessary   rough calculations sufficient

Exceptions: neutrino masses, dark matter, ...

In collider physics? $b \to s \ell^+ \ell^-$? $R_{D^{(*)}}$?

Ratios of exclusive semileptonic branching ratios

$R(D^{(*)}) = \mathcal{B}(B \to D^{(*)}\tau\bar{\nu})/\mathcal{B}(B \to D^{(*)}\mu\bar{\nu})$ (summer 2023):

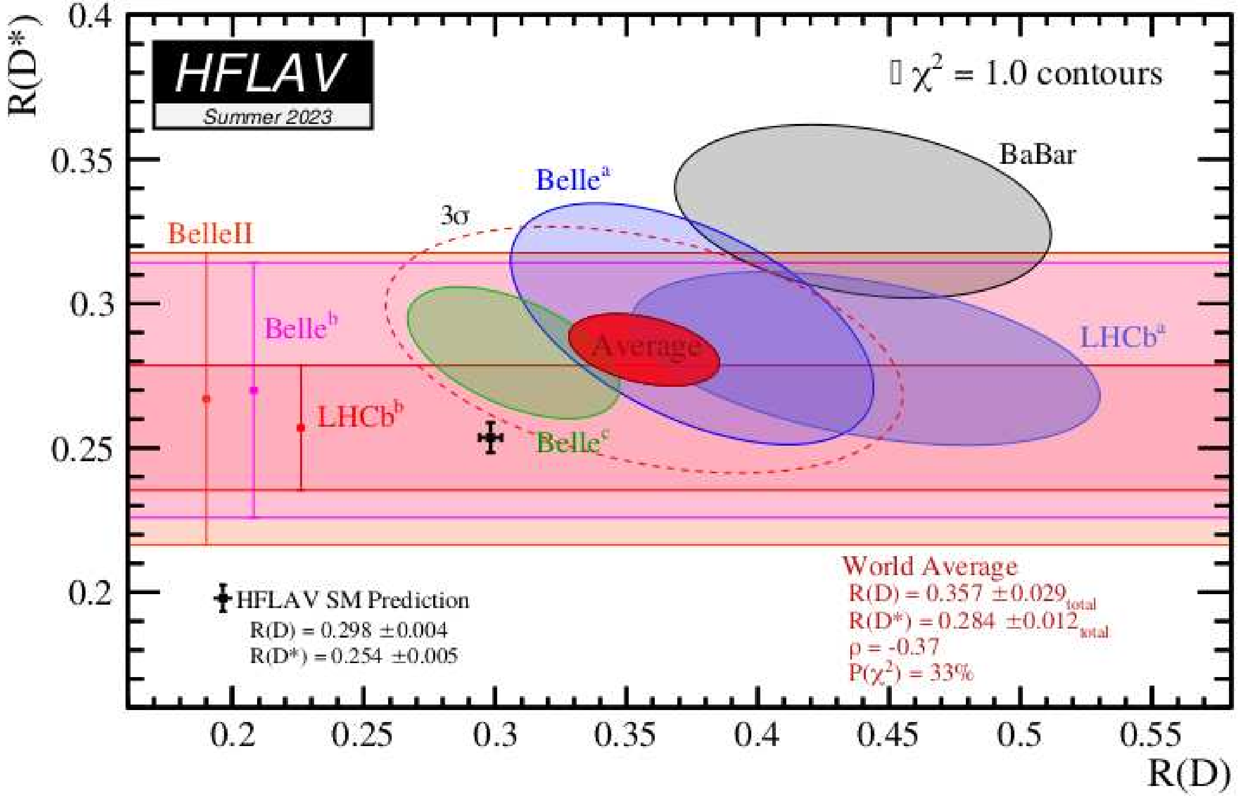

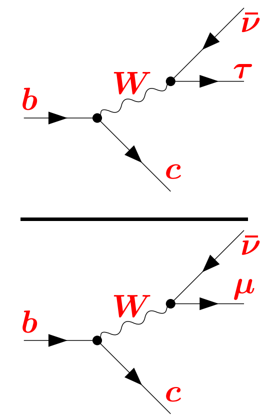

A $\sim 3.3\sigma$ deviation from the SM remains.

Large BSM effect or an experimental issue?

Deviations from SM predictions in $b \to s\ell^+\ell^-$ transitions?

Recent LHCb measurement of

$$R_{K^{(*)}} = \frac{\mathcal{B}(B \to K^{(*)}\mu^+\mu^-)}{\mathcal{B}(B \to K^{(*)}e^+e^-)}$$

[arXiv:2212.09153]

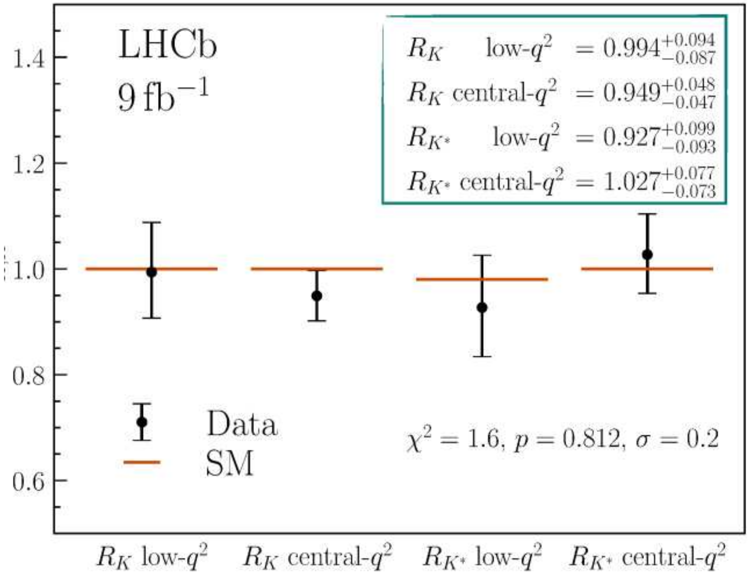

low q^2: $[0.1, 1, 1]$ GeV^2
central q^2: $[1.1, 6.0]$ GeV^2

Deviations from SM predictions in $b \to s\ell^+\ell^-$ transitions?

Recent LHCb measurement of

$$R_{K^{(*)}} = \frac{\mathcal{B}(B \to K^{(*)}\mu^+\mu^-)}{\mathcal{B}(B \to K^{(*)}e^+e^-)}$$

[arXiv:2212.09153]

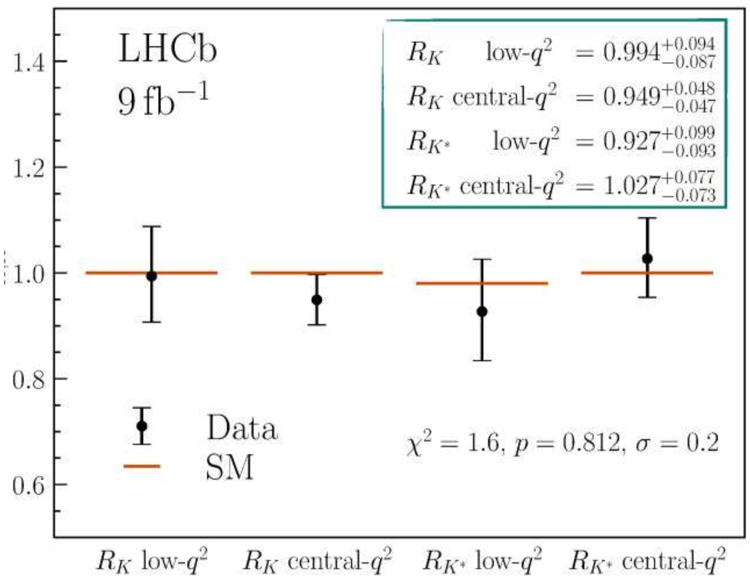

low q^2: $[0.1, 1, 1]$ GeV^2
central q^2: $[1.1, 6.0]$ GeV^2

Sample constraints on the *bsll* operator Wilson coefficients from arXiv:2212.10497 by A. Grelio, J. Salko, A. Smolkovič, P. Stangl:

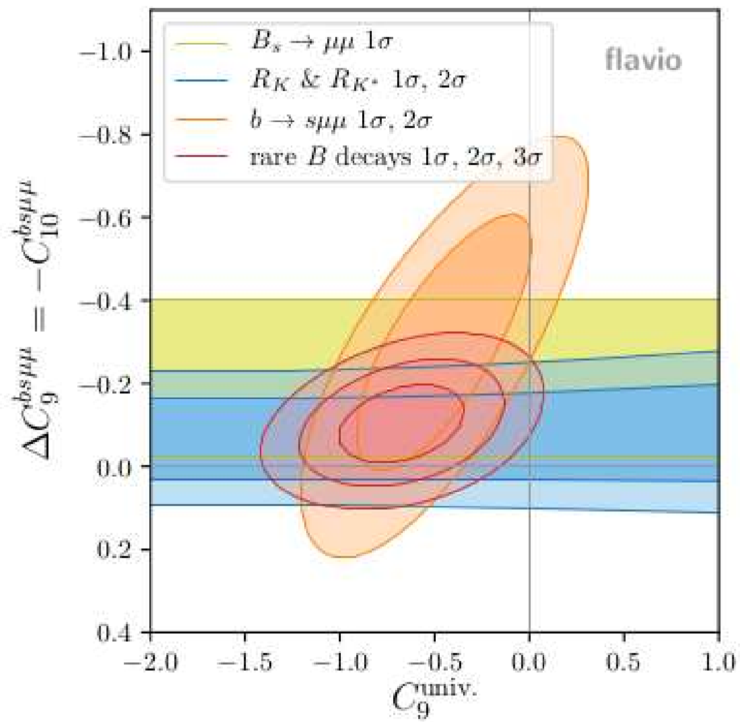

Deviations from SM predictions in $b \to s\ell^+\ell^-$ transitions?

Recent LHCb measurement of

$$R_{K^{(*)}} = \frac{\mathcal{B}(B\to K^{(*)}\mu^+\mu^-)}{\mathcal{B}(B\to K^{(*)}e^+e^-)}$$

[arXiv:2212.09153]

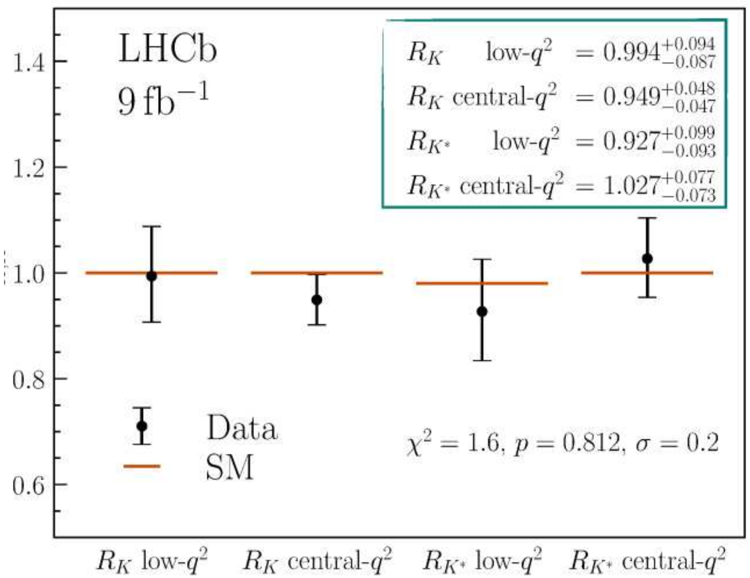

low q^2: $[0.1, 1, 1]$ GeV^2
central q^2: $[1.1, 6.0]$ GeV^2

Sample constraints on the *bsll* operator Wilson coefficients from arXiv:2212.10497 by A. Grelio, J. Salko, A. Smolkovič, P. Stangl:

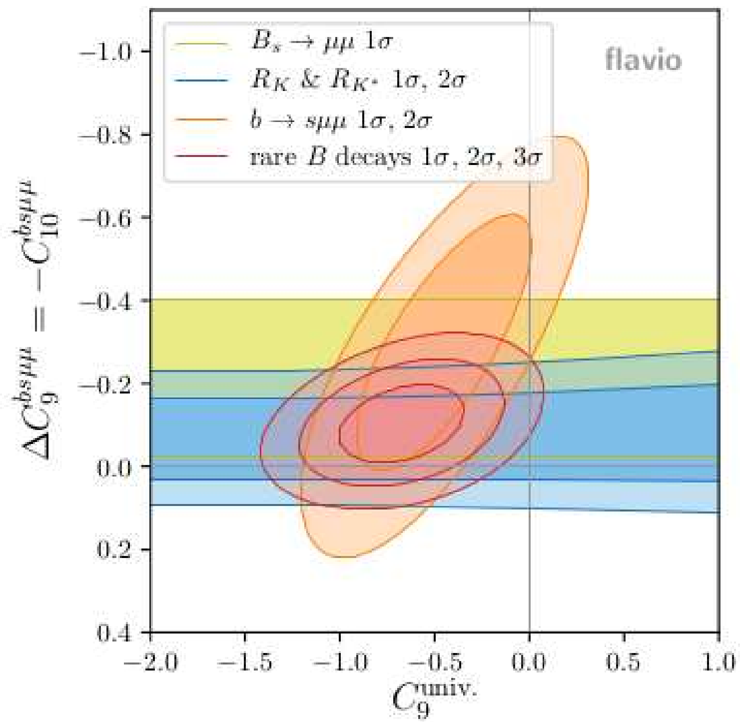

Possible charm-loop effects that could mimic a deviation in C_9^{univ}:

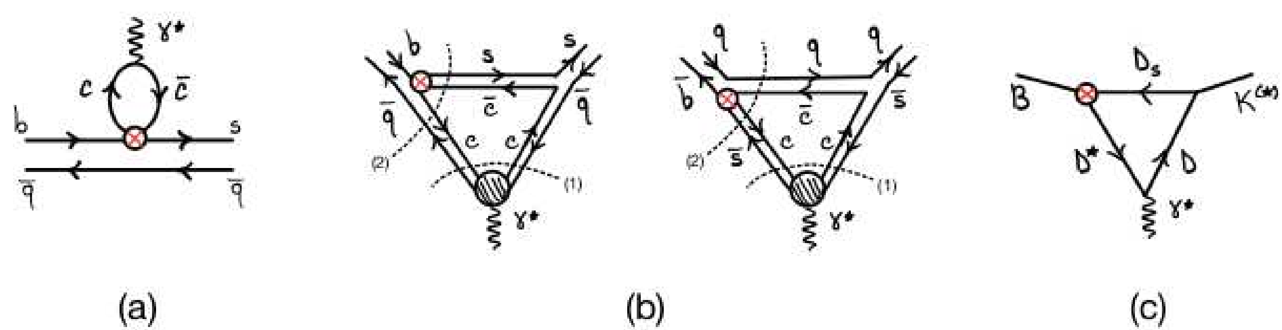

Fig. 1 from arXiv:2212.10516 by M. Ciuchini, M. Fedele, E. Franco, A. Paul, L. Silvestrini and M. Valli.

SM predictions vs. measurements for $\mathcal{B}(\bar{B} \to X_s\gamma)$ and $\mathcal{B}(B_s \to \mu^+\mu^-)$

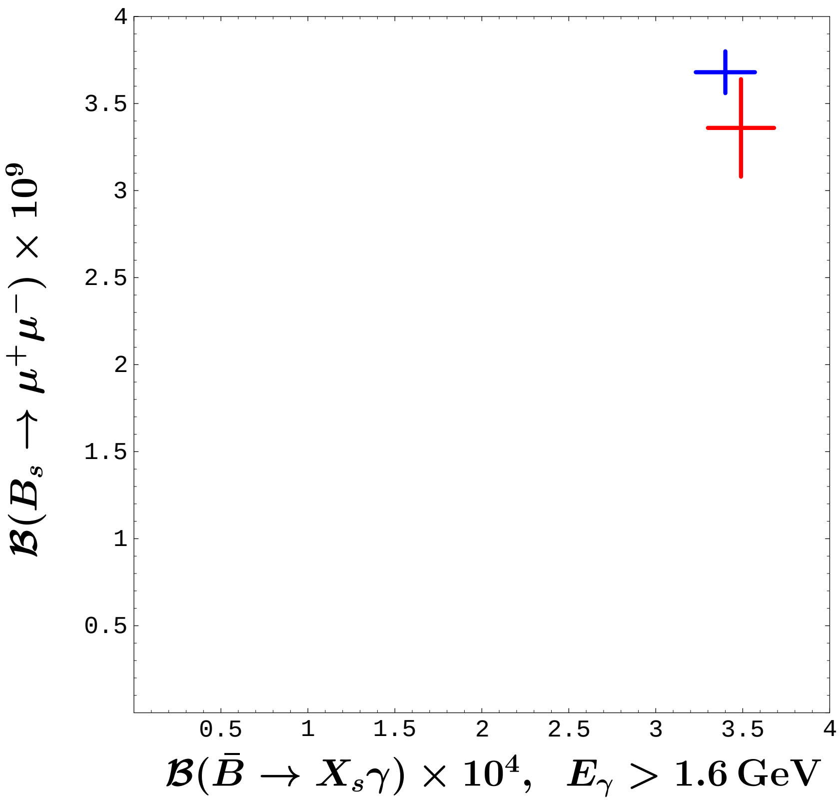

SM predictions vs. measurements for $\mathcal{B}(\bar{B} \to X_s\gamma)$ and $\mathcal{B}(B_s \to \mu^+\mu^-)$

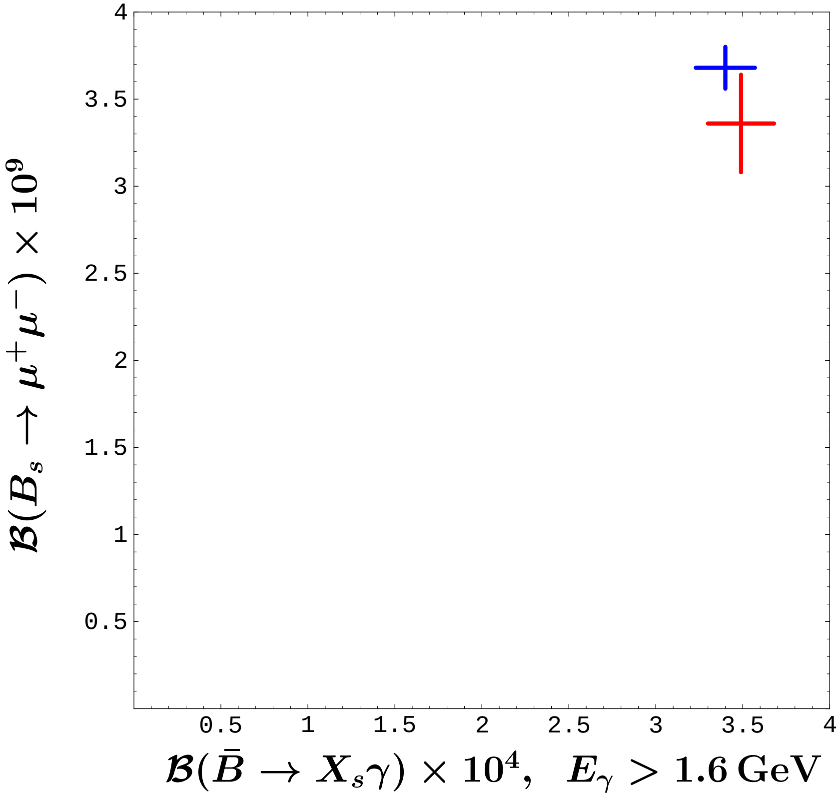

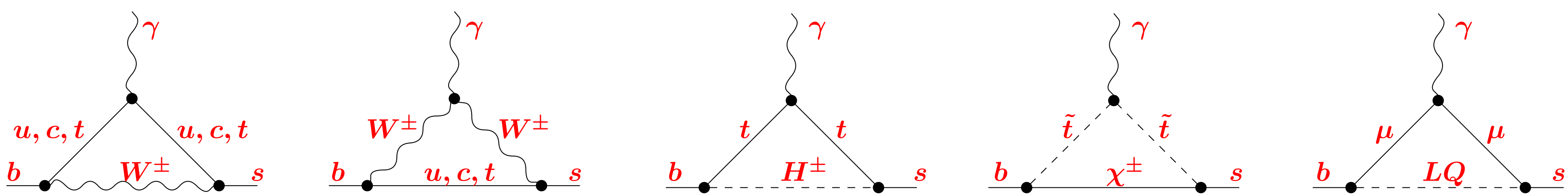

SM predictions vs. measurements for $\mathcal{B}(\bar{B} \to X_s \gamma)$ and $\mathcal{B}(B_s \to \mu^+ \mu^-)$

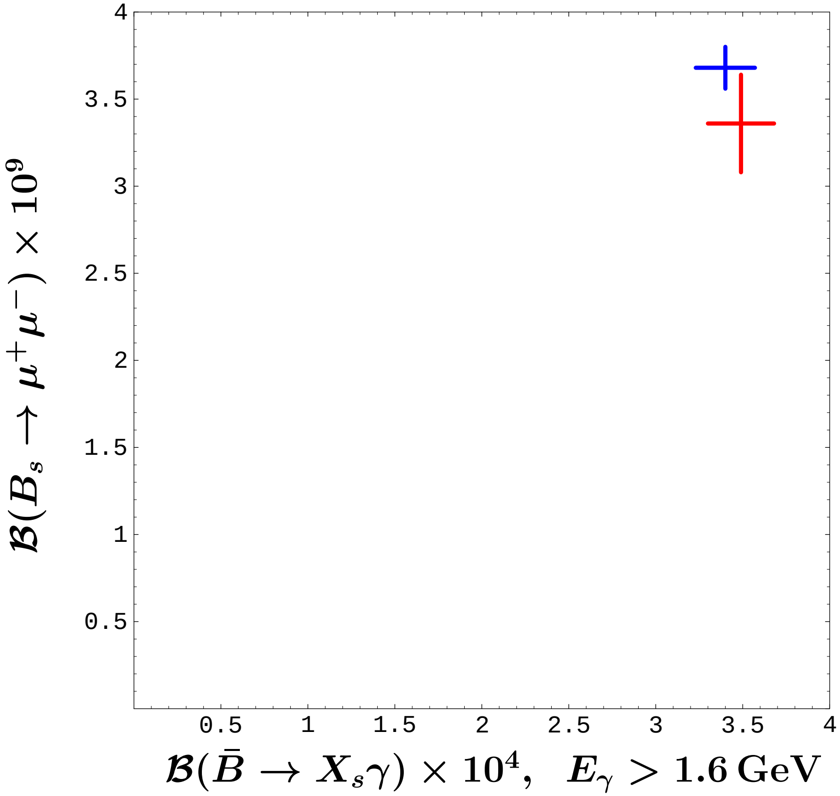

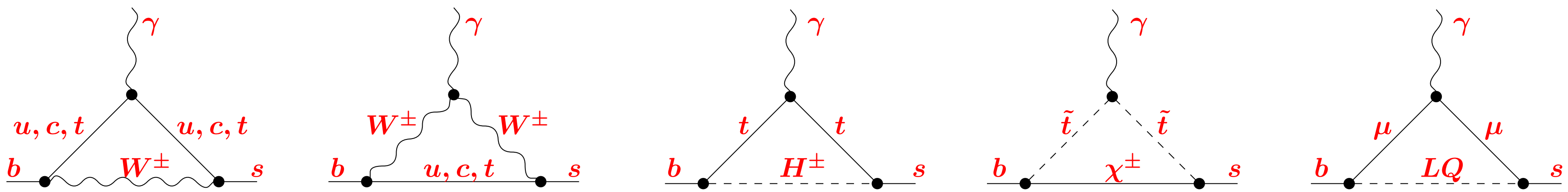

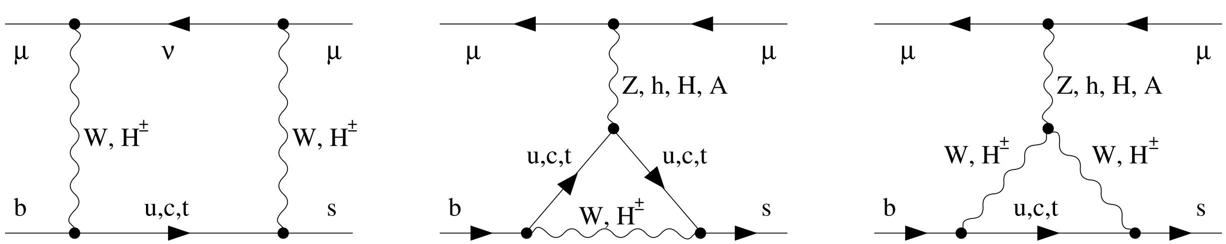

SM predictions vs. measurements for $\mathcal{B}(\bar{B} \to X_s\gamma)$ and $\mathcal{B}(B_s \to \mu^+\mu^-)$

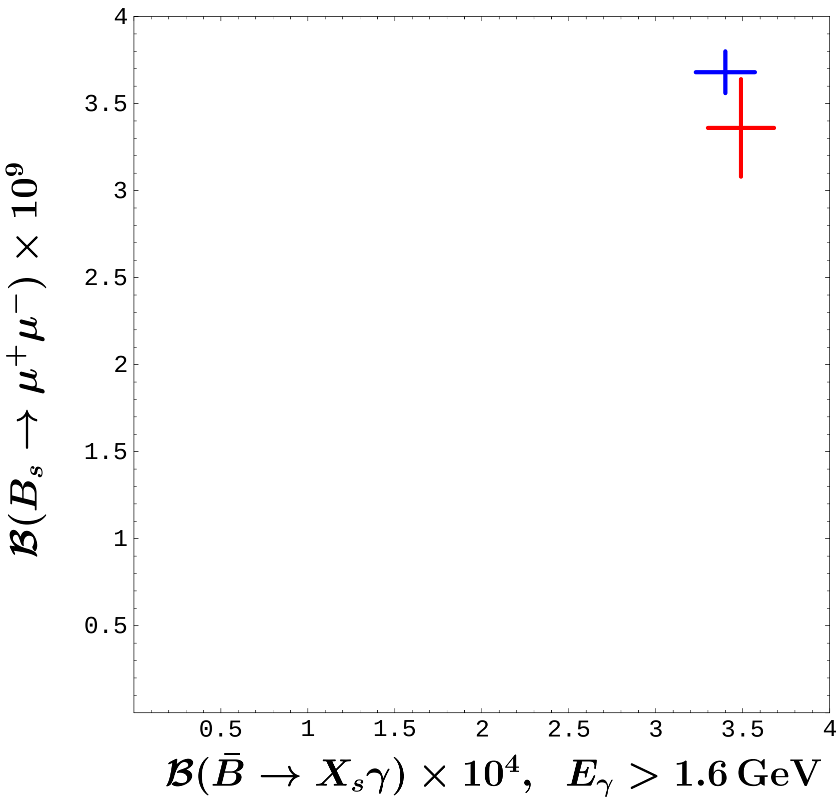

$\mathcal{B}(\bar{B} \to X_s\gamma)^{\text{exp}}_{E_\gamma>1.6} \times 10^4 = 3.49 \pm 0.19 \quad (\pm 5.4\%)$

CLEO, BaBar and Belle measurements combined by PDG [2022] and HFLAV [arXiv:2206.07501].

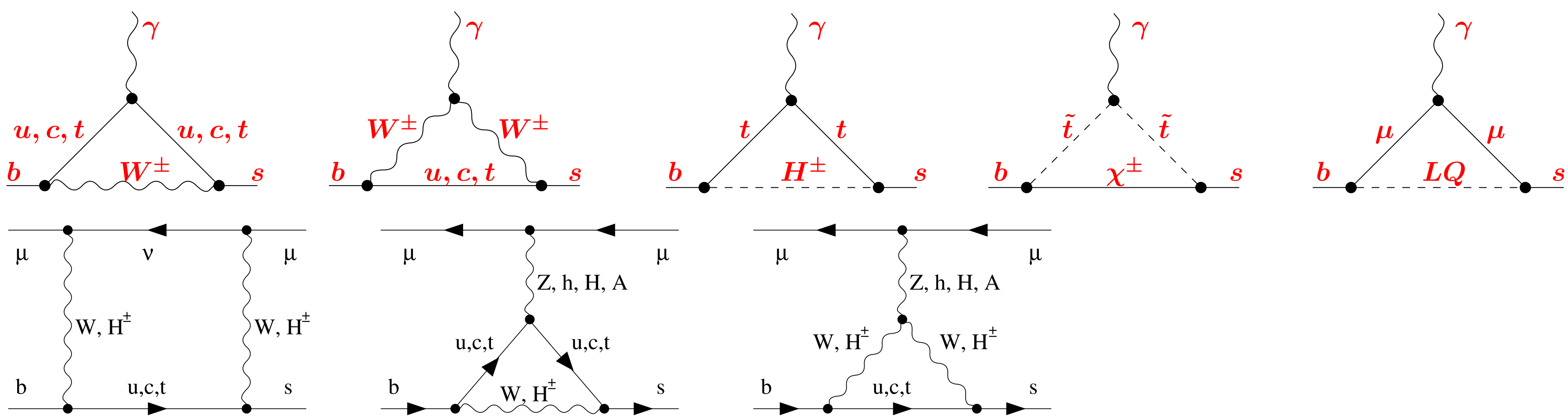

SM predictions vs. measurements for $\mathcal{B}(\bar{B} \to X_s\gamma)$ and $\mathcal{B}(B_s \to \mu^+\mu^-)$

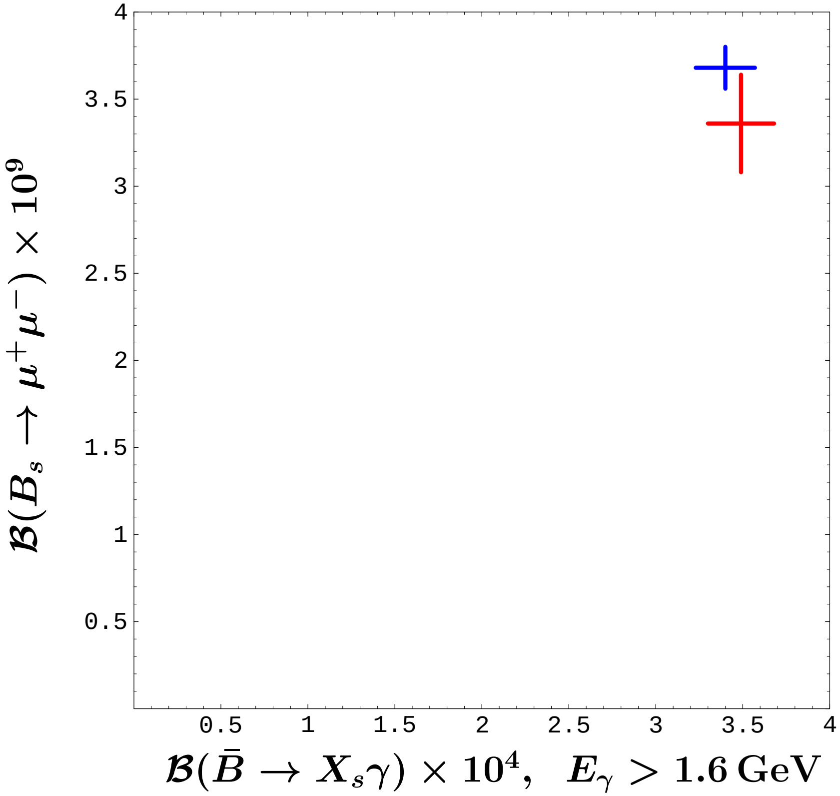

$\mathcal{B}(\bar{B} \to X_s\gamma)^{\mathrm{exp}}_{E_\gamma>1.6} \times 10^4 = 3.49 \pm 0.19 \quad (\pm 5.4\%)$

CLEO, BaBar and Belle measurements combined by PDG [2022] and HFLAV [arXiv:2206.07501].

$\mathcal{B}(\bar{B} \to X_s\gamma)^{\mathrm{SM}}_{E_\gamma>1.6} \times 10^4 = 3.40 \pm 0.17 \quad (\pm 5.0\%)$

arXiv:2002.01548 by MM, A. Rehman, M. Steinhauser.

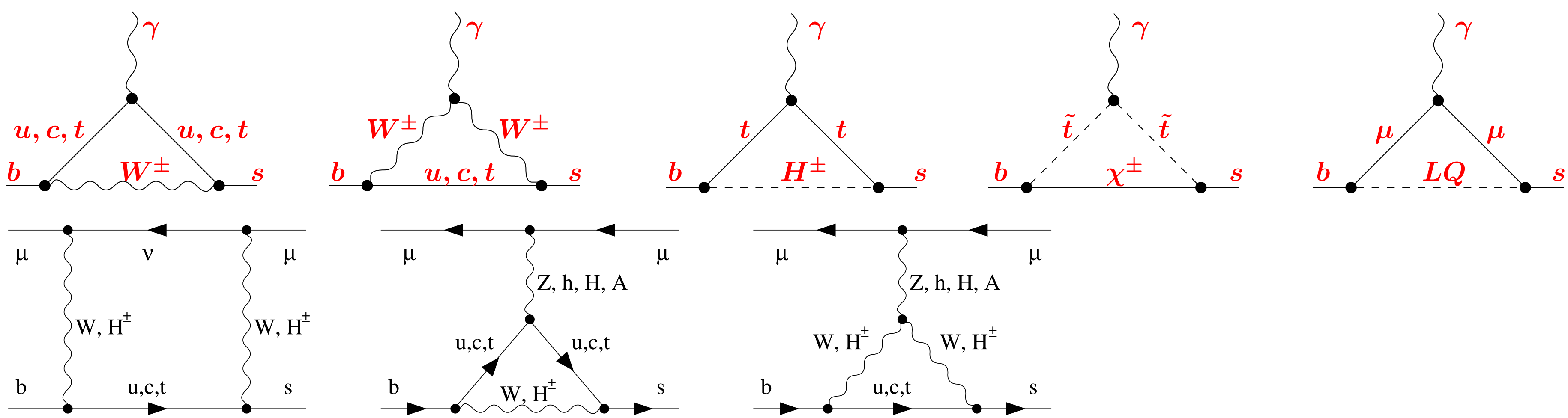

SM predictions vs. measurements for $\mathcal{B}(\bar{B} \to X_s\gamma)$ and $\mathcal{B}(B_s \to \mu^+\mu^-)$

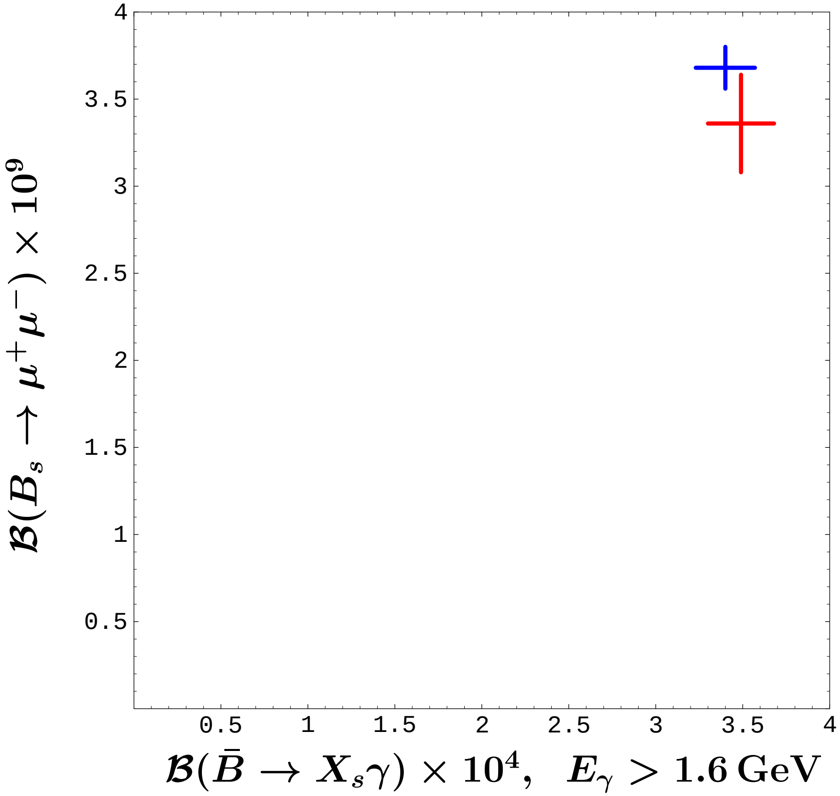

$$\mathcal{B}(\bar{B} \to X_s\gamma)^{\mathrm{exp}}_{E_\gamma > 1.6} \times 10^4 = 3.49 \pm 0.19 \quad (\pm 5.4\%)$$

CLEO, BaBar and Belle measurements combined by PDG [2022] and HFLAV [arXiv:2206.07501].

$$\mathcal{B}(\bar{B} \to X_s\gamma)^{\mathrm{SM}}_{E_\gamma > 1.6} \times 10^4 = 3.40 \pm 0.17 \quad (\pm 5.0\%)$$

arXiv:2002.01548 by MM, A. Rehman, M. Steinhauser.

$$\mathcal{B}(B_s \to \mu^+\mu^-)^{\mathrm{exp}} \times 10^9 = 3.36 \pm 0.28 \quad (\pm 8.3\%)$$

LHCb'21, CMS'22 and ATLAS'18 measurements combined in arXiv:2212.10497 by A. Greljo, J. Salko, A. Smolkovič, P. Stangl.

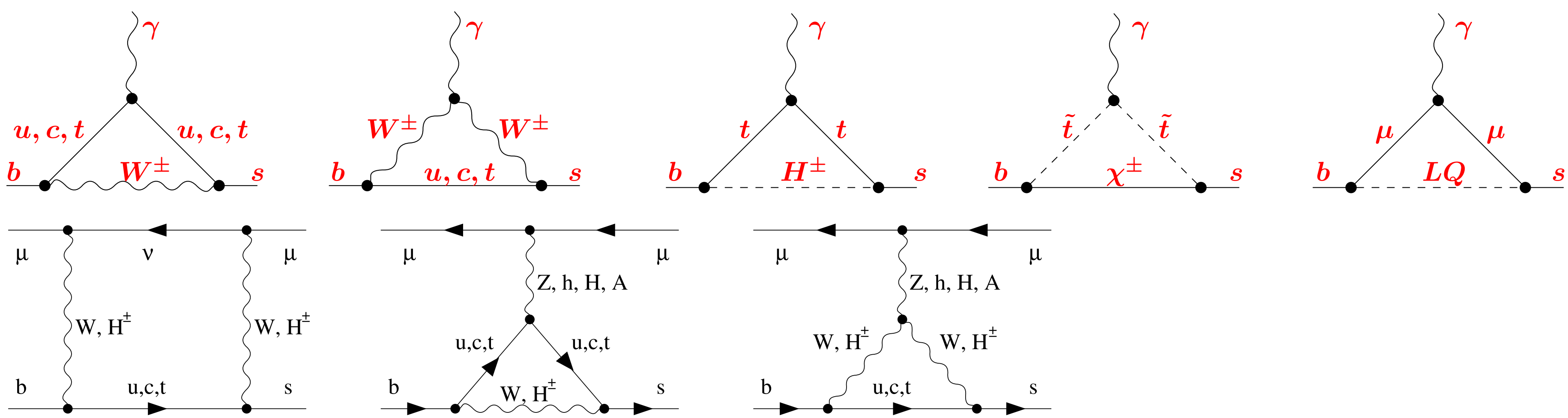

SM predictions vs. measurements for $\mathcal{B}(\bar{B} \to X_s\gamma)$ and $\mathcal{B}(B_s \to \mu^+\mu^-)$

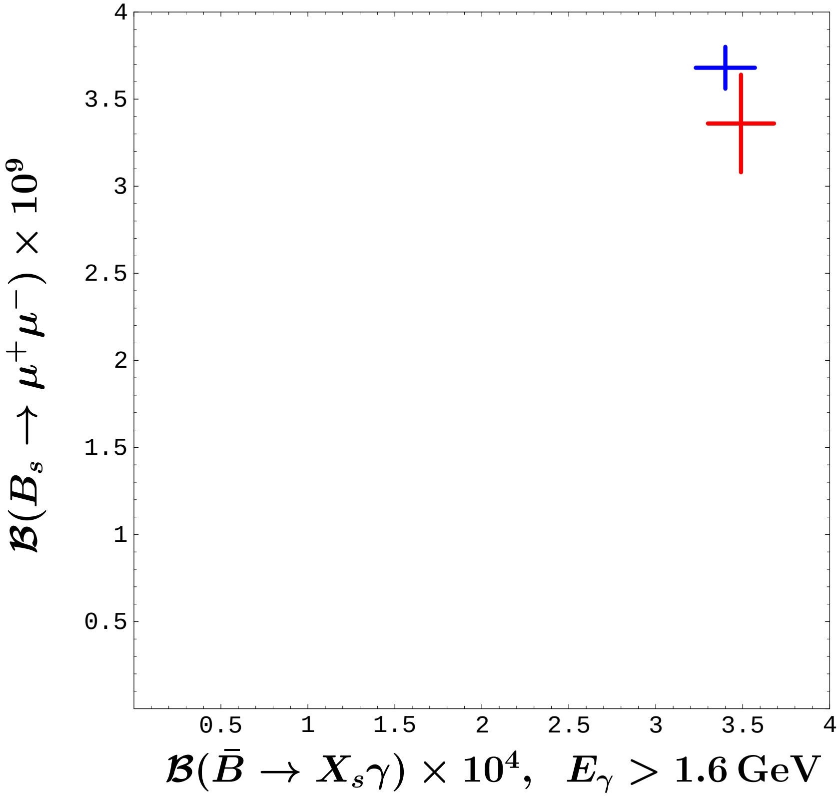

$\mathcal{B}(\bar{B} \to X_s\gamma)^{\mathrm{exp}}_{E_\gamma > 1.6} \times 10^4 = 3.49 \pm 0.19 \quad (\pm 5.4\%)$

CLEO, BaBar and Belle measurements combined by PDG [2022] and HFLAV [arXiv:2206.07501].

$\mathcal{B}(\bar{B} \to X_s\gamma)^{\mathrm{SM}}_{E_\gamma > 1.6} \times 10^4 = 3.40 \pm 0.17 \quad (\pm 5.0\%)$

arXiv:2002.01548 by MM, A. Rehman, M. Steinhauser.

$\mathcal{B}(B_s \to \mu^+\mu^-)^{\mathrm{exp}} \times 10^9 = 3.36 \pm 0.28 \quad (\pm 8.3\%)$

LHCb'21, CMS'22 and ATLAS'18 measurements combined in arXiv:2212.10497 by A. Greljo, J. Salko, A. Smolkovič, P. Stangl.

$\mathcal{B}(B_s \to \mu^+\mu^-)^{\mathrm{SM}} \times 10^9 = 3.68 \pm 0.12 \quad (\pm 3.2\%)$

arXiv:1311.0903 by C. Bobeth, M. Gorbahn, T. Hermann, MM, E. Stamou, M. Steinhauser with parameter updates (next slides) and -0.5% QED correction from arXiv:1907.07011 by M. Beneke, C. Bobeth and R. Szafron.

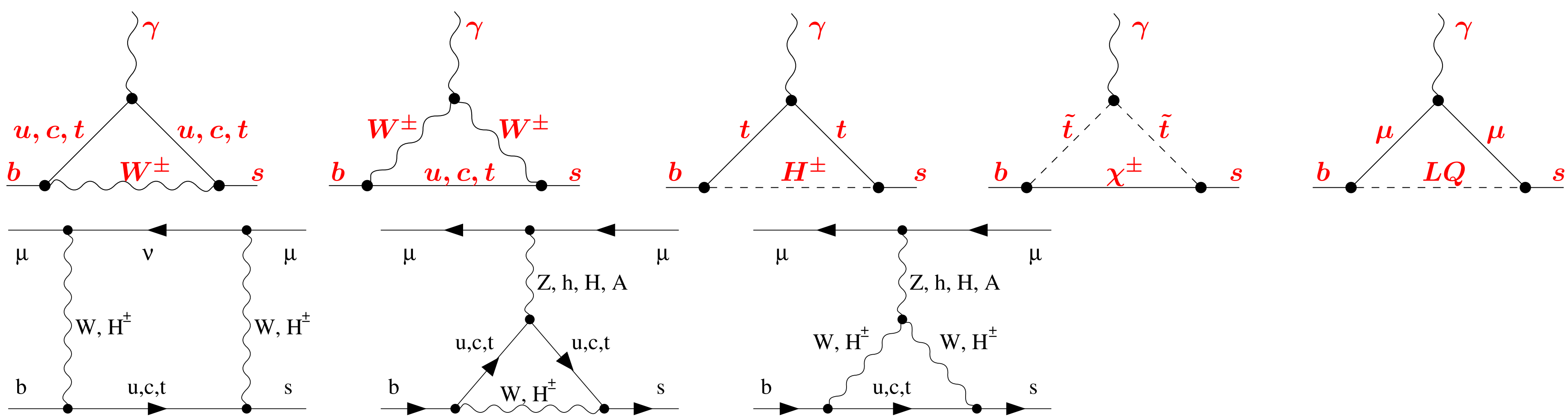

Input parameter update for $B_{s,d} \to \ell^+\ell^-$

	arXiv:1311.0903	this talk	source
M_t [GeV]	173.1(9)	172.69(30)	PDG'23, `https://pdglive.lbl.gov`
$\alpha_s(M_Z)$	0.1184(7)	0.1179(9)	PDG'22, `https://pdg.lbl.gov`
f_{B_s} [GeV]	0.2277(45)	0.2303(13)	FLAG'23, `http://flag.unibe.ch`
f_{B_d} [GeV]	0.1905(42)	0.1900(13)	FLAG'23, `http://flag.unibe.ch`
$\lvert V_{cb}\rvert \times 10^3$	42.40(90)	42.16(50)	inclusive, arXiv:2107.00604
$\lvert V_{tb}^* V_{ts}\rvert / \lvert V_{cb}\rvert$	0.9800(10)	0.9818(5)	derived from UT*fit*, arXiv:2212.03894
$\lvert V_{tb}^* V_{td}\rvert \times 10^2$	0.88(3)	0.859(11)	UT*fit*, arXiv:2212.03894
τ_H^s [ps]	1.615(21)	1.624(9)	HFLAV'23, `https://hflav.web.cern.ch`
τ_H^d [ps]	1.519(7)	1.519(4)	HFLAV'23, `https://hflav.web.cern.ch`
$\overline{\mathcal{B}}_{s\mu} \times 10^9$	3.65(23)	3.68(12)	
$\overline{\mathcal{B}}_{d\mu} \times 10^{10}$	1.06(9)	0.99(4)	

Sources of uncertainties	f_{B_q}	CKM	τ_H^q	M_t	α_s	other parametric	non-parametric	$\sum$
$\overline{\mathcal{B}}_{s\ell}$	1.1%	2.4%	0.6%	0.5%	0.2%	< 0.1%	1.5%	3.2%
$\overline{\mathcal{B}}_{d\ell}$	1.4%	2.6%	0.3%	0.5%	0.2%	< 0.1%	1.5%	3.6%

SM predictions for all the branching ratios $\overline{\mathcal{B}}_{q\ell} \equiv \overline{\mathcal{B}}(B_q^0 \to \ell^+\ell^-)$ including 2-loop electroweak and 3-loop QCD matching at $\mu_0 \sim m_t$

[C. Bobeth, M. Gorbahn, T. Hermann, MM, E. Stamou, M. Steinhauser, arXiv:1311.0903]

$$
\begin{aligned}
\overline{\mathcal{B}}_{se} \times 10^{14} &= \eta_{\rm QED}(8.54 \pm 0.13)\, R_{t\alpha}\, R_s, \\
\overline{\mathcal{B}}_{s\mu} \times 10^{9} &= \eta_{\rm QED}(3.65 \pm 0.06)\, R_{t\alpha}\, R_s, \\
\overline{\mathcal{B}}_{s\tau} \times 10^{7} &= \eta_{\rm QED}(7.73 \pm 0.12)\, R_{t\alpha}\, R_s, \\
\overline{\mathcal{B}}_{de} \times 10^{15} &= \eta_{\rm QED}(2.48 \pm 0.04)\, R_{t\alpha}\, R_d, \\
\overline{\mathcal{B}}_{d\mu} \times 10^{10} &= \eta_{\rm QED}(1.06 \pm 0.02)\, R_{t\alpha}\, R_d, \\
\overline{\mathcal{B}}_{d\tau} \times 10^{8} &= \eta_{\rm QED}(2.22 \pm 0.04)\, R_{t\alpha}\, R_d,
\end{aligned}
$$

where

$$
\begin{aligned}
R_{t\alpha} &= \left(\frac{M_t}{173.1\ \text{GeV}}\right)^{3.06} \left(\frac{\alpha_s(M_Z)}{0.1184}\right)^{-0.18}, \\
R_s &= \left(\frac{f_{B_s}[\text{MeV}]}{227.7}\right)^2 \left(\frac{|V_{cb}|}{0.0424}\right)^2 \left(\frac{|V_{tb}^\star V_{ts}/V_{cb}|}{0.980}\right)^2 \frac{\tau_H^s\ [\text{ps}]}{1.615}, \\
R_d &= \left(\frac{f_{B_d}[\text{MeV}]}{190.5}\right)^2 \left(\frac{|V_{tb}^\star V_{td}|}{0.0088}\right)^2 \frac{\tau_d^{\rm av}\ [\text{ps}]}{1.519}.
\end{aligned}
$$

Enhanced QED effects in $B_q \to \ell^+\ell^-$

The leading contribution to the decay rate is suppressed by $\frac{m_\ell^2}{M_{B_q}^2}$.

Enhanced QED effects in $B_q \to \ell^+\ell^-$

The leading contribution to the decay rate is suppressed by $\frac{m_\ell^2}{M_{B_q}^2}$.

As observed by M. Beneke, C. Bobeth and R. Szafron in arXiv:1708.09152,

some of the QED corrections receive suppression by $\frac{m_\ell^2}{\Lambda M_{B_q}}$ only:

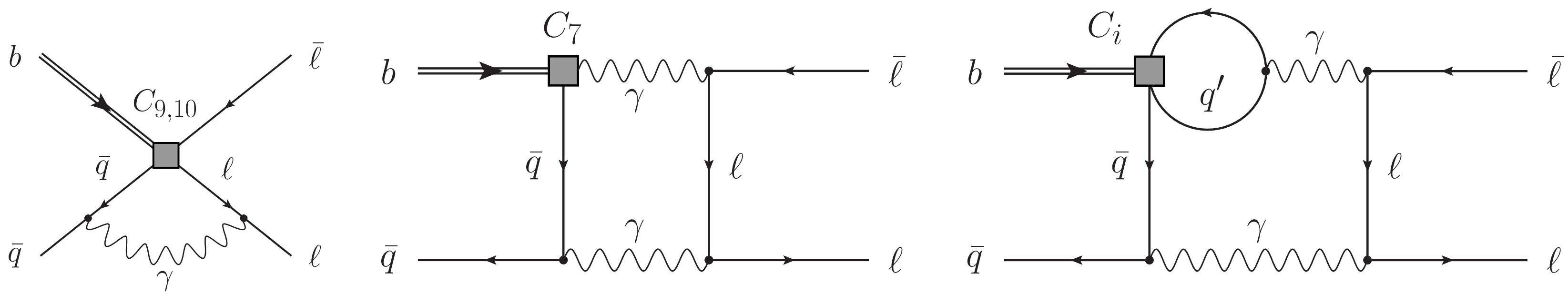

See also the lecture by RS at the Paris-2019 workshop:
`https://indico.in2p3.fr/event/18845/sessions/12137/attachments/54326/71064/Szafron.pdf`

Enhanced QED effects in $B_q \to \ell^+\ell^-$

The leading contribution to the decay rate is suppressed by $\frac{m_\ell^2}{M_{B_q}^2}$.

As observed by M. Beneke, C. Bobeth and R. Szafron in arXiv:1708.09152,

some of the QED corrections receive suppression by $\frac{m_\ell^2}{\Lambda M_{B_q}}$ only:

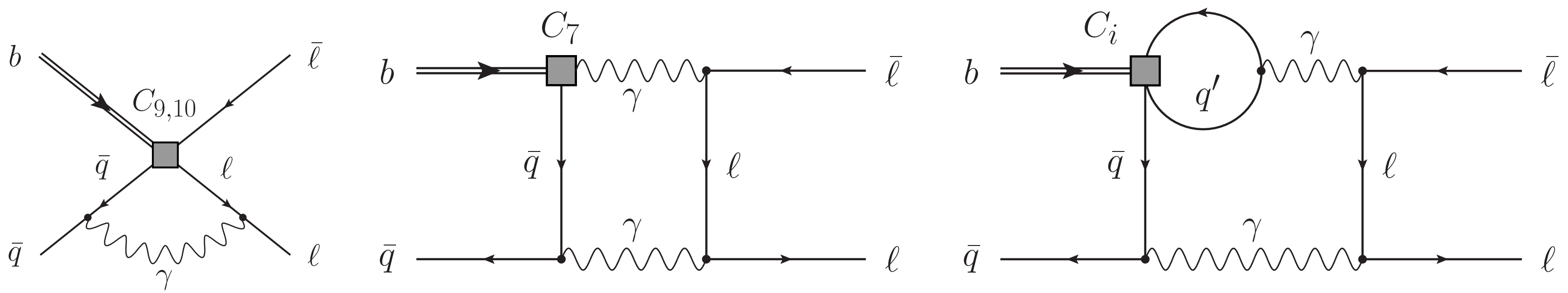

See also the lecture by RS at the Paris-2019 workshop:
`https://indico.in2p3.fr/event/18845/sessions/12137/attachments/54326/71064/Szafron.pdf`

Consequently, the relative QED correction scales like $\frac{\alpha_{em}}{\pi} \frac{M_{B_q}}{\Lambda}$.

Enhanced QED effects in $B_q \to \ell^+\ell^-$

The leading contribution to the decay rate is suppressed by $\frac{m_\ell^2}{M_{B_q}^2}$.

As observed by M. Beneke, C. Bobeth and R. Szafron in arXiv:1708.09152, some of the QED corrections receive suppression by $\frac{m_\ell^2}{\Lambda M_{B_q}}$ only:

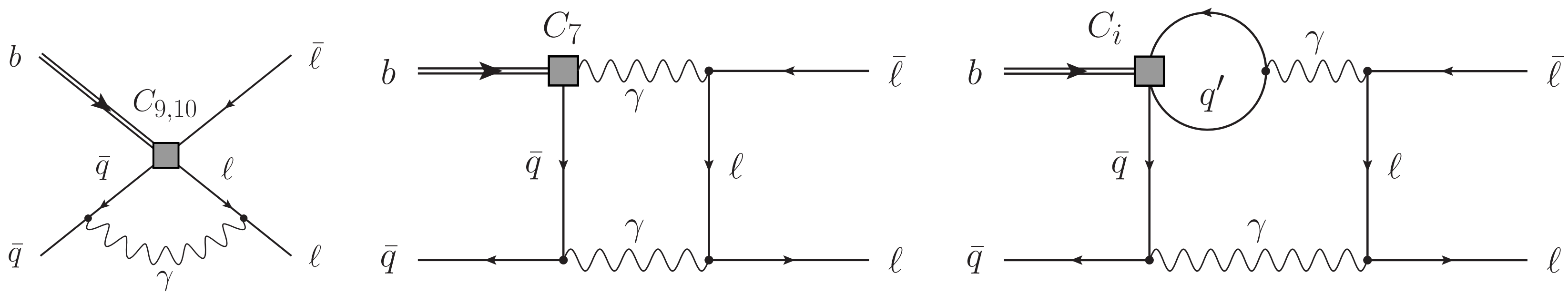

See also the lecture by RS at the Paris-2019 workshop:
`https://indico.in2p3.fr/event/18845/sessions/12137/attachments/54326/71064/Szafron.pdf`

Consequently, the relative QED correction scales like $\frac{\alpha_{em}}{\pi}\frac{M_{B_q}}{\Lambda}$.

Their explicit calculation in arXiv:1908.07011 implies that the previous results for all the $B_q \to \ell^+\ell^-$ branching ratios need to be multiplied by

$$\eta_{\rm QED} = 0.995^{+0.03}_{-0.05}.$$

Enhanced QED effects in $B_q \to \ell^+\ell^-$

The leading contribution to the decay rate is suppressed by $\frac{m_\ell^2}{M_{B_q}^2}$.

As observed by M. Beneke, C. Bobeth and R. Szafron in arXiv:1708.09152,

some of the QED corrections receive suppression by $\frac{m_\ell^2}{\Lambda M_{B_q}}$ only:

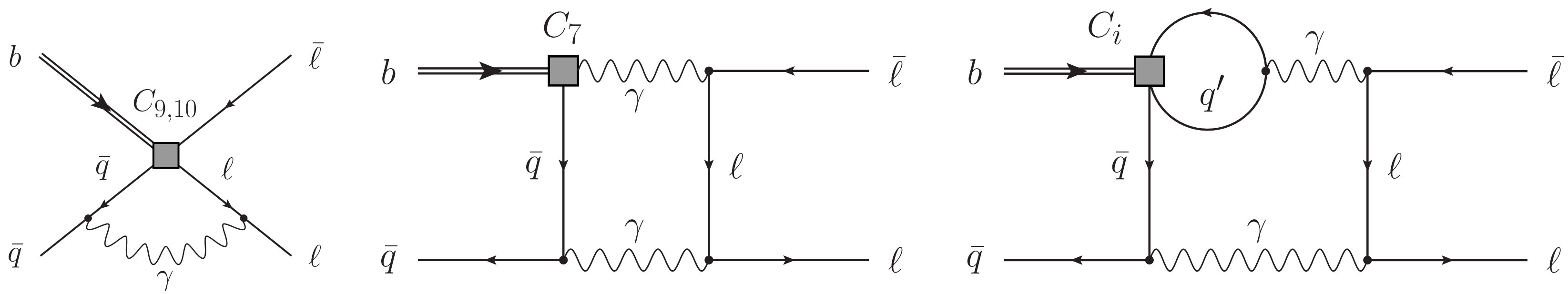

See also the lecture by RS at the Paris-2019 workshop:
`https://indico.in2p3.fr/event/18845/sessions/12137/attachments/54326/71064/Szafron.pdf`

Consequently, the relative QED correction scales like $\frac{\alpha_{em}}{\pi}\frac{M_{B_q}}{\Lambda}$.

Their explicit calculation in arXiv:1908.07011 implies that the previous results for all the $B_q \to \ell^+\ell^-$ branching ratios need to be multiplied by

$$\eta_{\rm QED} = 0.995^{+0.03}_{-0.05}.$$

Thus, despite the $\frac{M_{B_q}}{\Lambda}$ -enhancement, the effect is well within the previously estimated $\pm 1.5\%$ non-parametric uncertainty.

Enhanced QED effects in $B_q \to \ell^+\ell^-$

The leading contribution to the decay rate is suppressed by $\frac{m_\ell^2}{M_{B_q}^2}$.

As observed by M. Beneke, C. Bobeth and R. Szafron in arXiv:1708.09152,

some of the QED corrections receive suppression by $\frac{m_\ell^2}{\Lambda M_{B_q}}$ only:

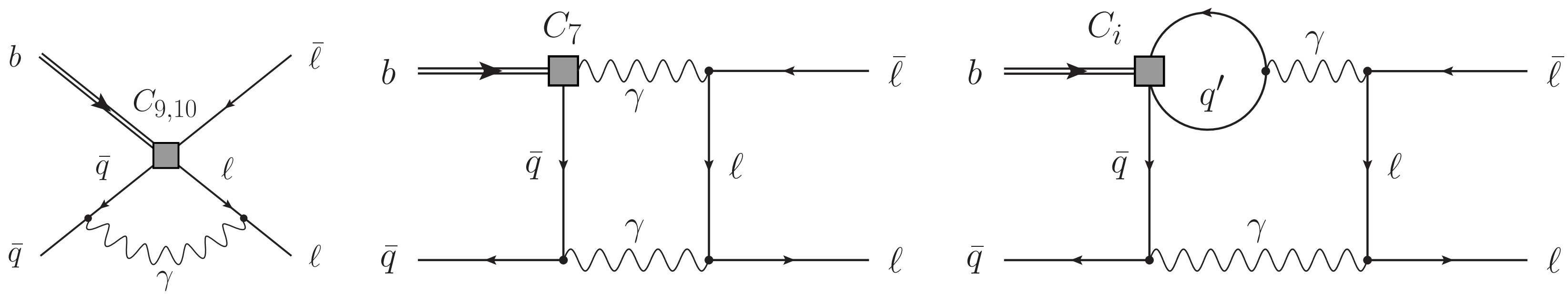

See also the lecture by RS at the Paris-2019 workshop:
`https://indico.in2p3.fr/event/18845/sessions/12137/attachments/54326/71064/Szafron.pdf`

Consequently, the relative QED correction scales like $\frac{\alpha_{em}}{\pi} \frac{M_{B_q}}{\Lambda}$.

Their explicit calculation in arXiv:1908.07011 implies that the previous results for all the $B_q \to \ell^+\ell^-$ branching ratios need to be multiplied by

$$\eta_{\rm QED} = 0.995^{+0.03}_{-0.05}.$$

Thus, despite the $\frac{M_{B_q}}{\Lambda}$ -enhancement, the effect is well within the previously estimated $\pm 1.5\%$ non-parametric uncertainty.

However, it is larger than $\pm 0.3\%$ due to scale-variation of the Wilson coefficient $C_A(\mu_b)$.

Determination of $\mathcal{B}(\bar{B} \to X_s\gamma)$ in the SM:

$$\mathcal{B}(\bar{B} \to X_s\gamma)_{E_\gamma > E_0} = \mathcal{B}(\bar{B} \to X_c e\bar{\nu})_{\rm exp} \left|\frac{V_{ts}^* V_{tb}}{V_{cb}}\right|^2 \frac{6\alpha_{\rm em}}{\pi\, \mathrm{C}} \Big[\underbrace{\mathrm{P}(\mathrm{E}_0)}_{\substack{\text{pert.}\\ \sim 96\%}} + \underbrace{N(E_0)}_{\substack{\text{non-pert.}\\ \sim 4\%}}\Big]$$

$$\frac{\Gamma[b \to X_s^p \gamma]_{E_\gamma > E_0}}{|V_{cb}/V_{ub}|^2\, \Gamma[b \to X_u^p e\bar{\nu}]} = \left|\frac{V_{ts}^* V_{tb}}{V_{cb}}\right|^2 \frac{6\alpha_{\rm em}}{\pi}\, \mathrm{P}(\mathrm{E}_0)$$

$$\mathrm{C} = \left|\frac{V_{ub}}{V_{cb}}\right|^2 \frac{\Gamma[\bar{B} \to X_c e\bar{\nu}]}{\Gamma[\bar{B} \to X_u e\bar{\nu}]}$$

semileptonic phase-space factor

Determination of $\mathcal{B}(\bar{B} \to X_s\gamma)$ in the SM:

$$\mathcal{B}(\bar{B} \to X_s\gamma)_{E_\gamma > E_0} = \mathcal{B}(\bar{B} \to X_c e\bar{\nu})_{\rm exp} \left| \frac{V_{ts}^* V_{tb}}{V_{cb}} \right|^2 \frac{6\alpha_{\rm em}}{\pi\, C} \left[\underset{\substack{\text{pert.} \\ \sim 96\%}}{P(E_0)} + \underset{\substack{\text{non-pert.} \\ \sim 4\%}}{N(E_0)} \right]$$

$$\frac{\Gamma[b \to X_s^p \gamma]_{E_\gamma > E_0}}{|V_{cb}/V_{ub}|^2\, \Gamma[b \to X_u^p e\bar{\nu}]} = \left| \frac{V_{ts}^* V_{tb}}{V_{cb}} \right|^2 \frac{6\alpha_{\rm em}}{\pi} P(E_0) \qquad\qquad C = \left| \frac{V_{ub}}{V_{cb}} \right|^2 \frac{\Gamma[\bar{B} \to X_c e\bar{\nu}]}{\Gamma[\bar{B} \to X_u e\bar{\nu}]}$$

semileptonic phase-space factor

Eight operators Q_i matter for $\mathcal{B}_{s\gamma}^{\rm SM}$ when the NLO EW and/or CKM-suppressed effects are neglected:

$Q_{1,2}$	Q_7	Q_8	$Q_{3,4,5,6}$
current-current	photonic dipole	gluonic dipole	penguin

Determination of $\mathcal{B}(\bar{B} \to X_s\gamma)$ in the SM:

$$\mathcal{B}(\bar{B} \to X_s\gamma)_{E_\gamma > E_0} = \mathcal{B}(\bar{B} \to X_c e\bar{\nu})_{\rm exp} \left|\frac{V_{ts}^* V_{tb}}{V_{cb}}\right|^2 \frac{6\alpha_{\rm em}}{\pi\, C} \left[\underbrace{P(E_0)}_{\substack{\text{pert.}\\ \sim 96\%}} + \underbrace{N(E_0)}_{\substack{\text{non-pert.}\\ \sim 4\%}}\right]$$

$$\frac{\Gamma[b \to X_s^p\gamma]_{E_\gamma > E_0}}{|V_{cb}/V_{ub}|^2\, \Gamma[b \to X_u^p e\bar{\nu}]} = \left|\frac{V_{ts}^* V_{tb}}{V_{cb}}\right|^2 \frac{6\alpha_{\rm em}}{\pi} P(E_0)$$

$$C = \left|\frac{V_{ub}}{V_{cb}}\right|^2 \frac{\Gamma[\bar{B} \to X_c e\bar{\nu}]}{\Gamma[\bar{B} \to X_u e\bar{\nu}]}$$

semileptonic phase-space factor

Eight operators Q_i matter for $\mathcal{B}_{s\gamma}^{\rm SM}$ when the NLO EW and/or CKM-suppressed effects are neglected:

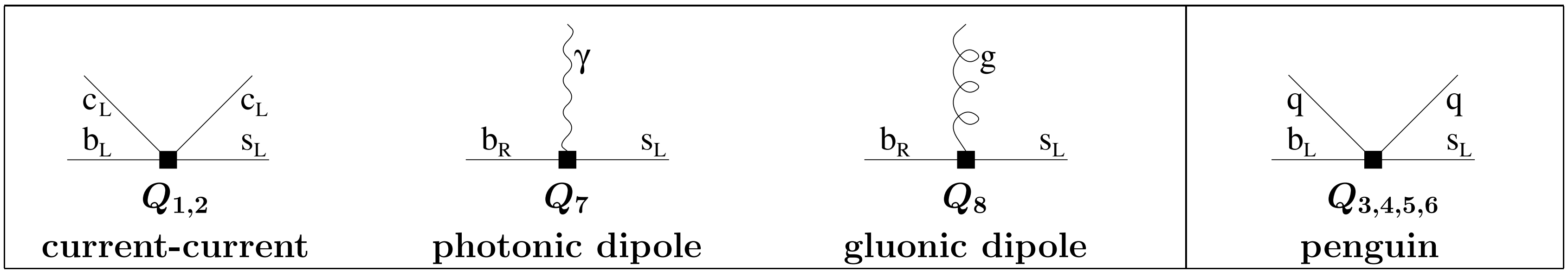

$$\Gamma(b \to X_s^p\gamma) = \frac{G_F^2\, m_{b,\,\rm pole}^5\, \alpha_{em}}{32\pi^4} \left|V_{ts}^* V_{tb}\right|^2 \sum_{i,j=1}^{8} C_i(\mu_b) C_j(\mu_b) \hat{G}_{ij}, \qquad (\hat{G}_{ij} = \hat{G}_{ji})$$

Determination of $\mathcal{B}(\bar{B} \to X_s\gamma)$ in the SM:

$$\mathcal{B}(\bar{B} \to X_s\gamma)_{E_\gamma > E_0} = \mathcal{B}(\bar{B} \to X_c e\bar{\nu})_{\rm exp} \left| \frac{V_{ts}^* V_{tb}}{V_{cb}} \right|^2 \frac{6\alpha_{\rm em}}{\pi\, C} \left[\underbrace{P(E_0)}_{\substack{\text{pert.} \\ \sim 96\%}} + \underbrace{N(E_0)}_{\substack{\text{non-pert.} \\ \sim 4\%}} \right]$$

$$\frac{\Gamma[b \to X_s^p\gamma]_{E_\gamma > E_0}}{|V_{cb}/V_{ub}|^2\, \Gamma[b \to X_u^p e\bar{\nu}]} = \left| \frac{V_{ts}^* V_{tb}}{V_{cb}} \right|^2 \frac{6\alpha_{\rm em}}{\pi} P(E_0)$$

$$C = \left| \frac{V_{ub}}{V_{cb}} \right|^2 \frac{\Gamma[\bar{B} \to X_c e\bar{\nu}]}{\Gamma[\bar{B} \to X_u e\bar{\nu}]}$$

semileptonic phase-space factor

Eight operators Q_i matter for $\mathcal{B}_{s\gamma}^{\rm SM}$ when the NLO EW and/or CKM-suppressed effects are neglected:

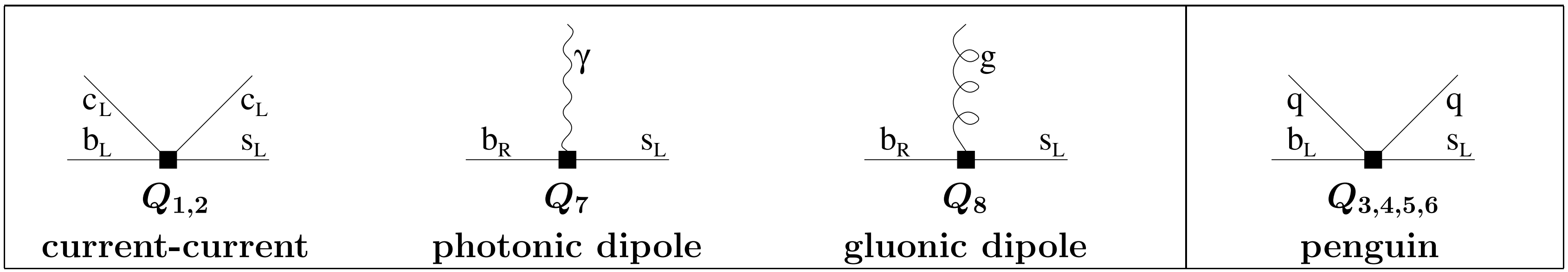

$$\Gamma(b \to X_s^p\gamma) = \frac{G_F^2\, m_{b,\,\rm pole}^5\, \alpha_{\rm em}}{32\pi^4} \left| V_{ts}^* V_{tb} \right|^2 \sum_{i,j=1}^{8} C_i(\mu_b) C_j(\mu_b) \hat{G}_{ij}, \qquad (\hat{G}_{ij} = \hat{G}_{ji})$$

NLO ($\mathcal{O}(\alpha_s)$) – last missing pieces being evaluated by Tobias Huber and Lars-Thorben Moos [arXiv:1912.07916]

Most important @ NNLO ($\mathcal{O}(\alpha_s^2)$): $\hat{G}_{77}$, $\hat{G}_{17}$, $\hat{G}_{27}$

$\hat{G}_{77}$: known

$\hat{G}_{17}$, $\hat{G}_{27}$: interpolated between the $m_c \gg m_b$ and $m_c = 0$ limits [arXiv:1503.01791]

$\Rightarrow \quad \pm 3\%$ uncertainty in $\mathcal{B}_{s\gamma}^{\rm SM}$

Sample diagrams contributing to $\hat{G}_{27}$ @ NNLO:

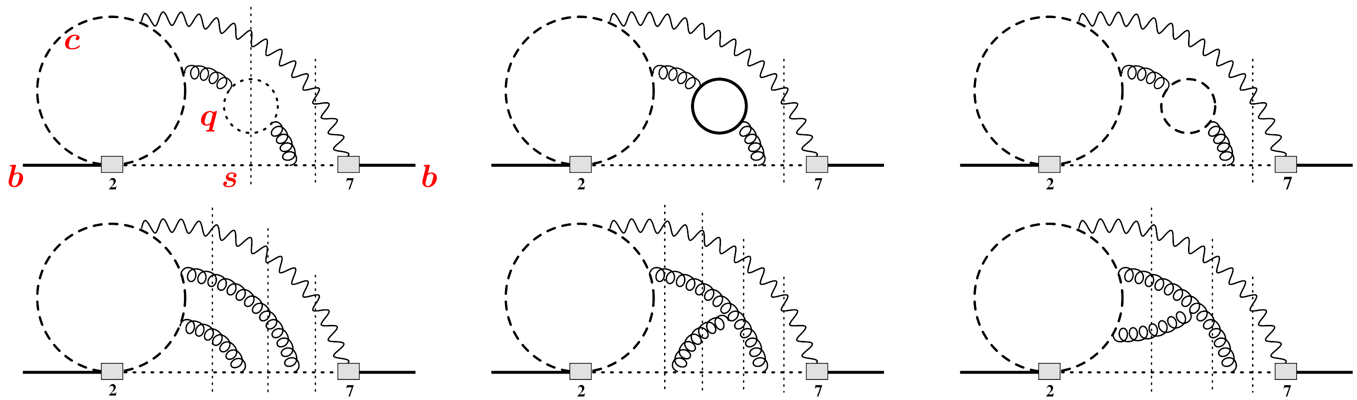

Sample diagrams contributing to $\hat{G}_{27}$ @ NNLO:

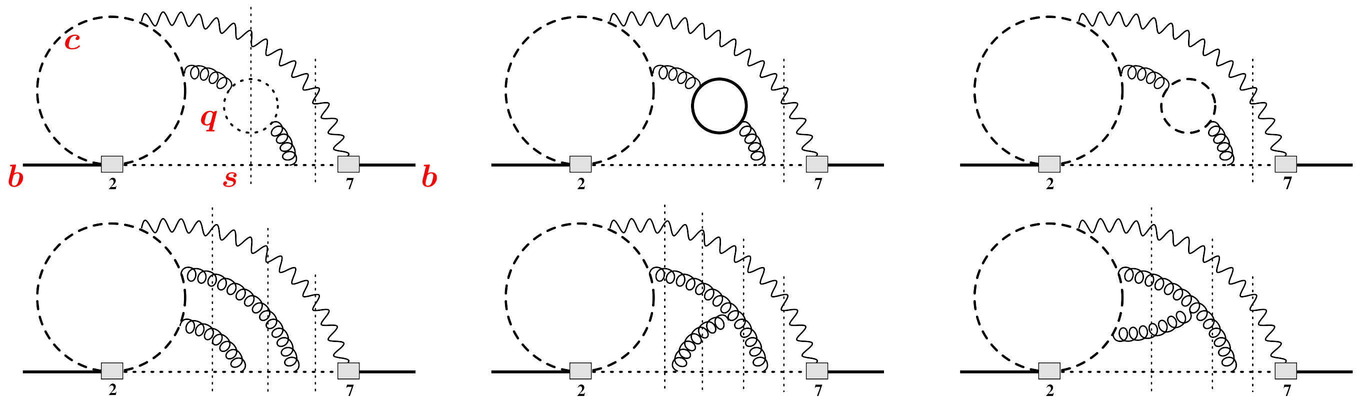

1. Generation of diagrams and performing the Dirac algebra to express everything in terms of (a few) $\times 10^5$ four-loop two-scale scalar integrals with unitarity cuts ($\mathcal{O}(500)$ families).

Sample diagrams contributing to $\hat{G}_{27}$ @ NNLO:

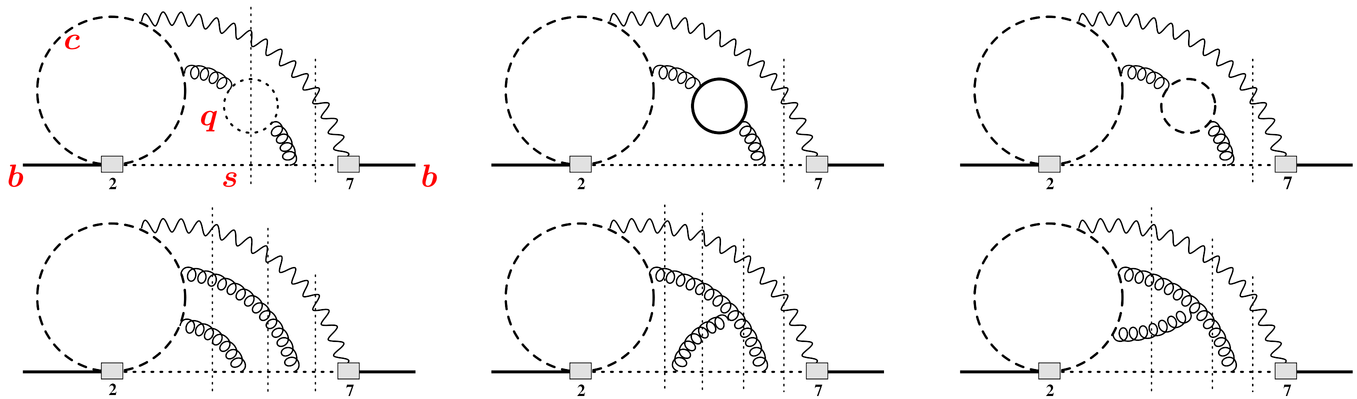

1. Generation of diagrams and performing the Dirac algebra to express everything in terms of (a few) $\times 10^5$ four-loop two-scale scalar integrals with unitarity cuts ($\mathcal{O}(500)$ families).

2. Reduction to master integrals (MIs) with the help of Integration By Parts (IBP) [KIRA]. $\mathcal{O}(1\,\mathrm{TB})$ RAM and weeks of CPU needed for the most complicated families.

Sample diagrams contributing to $\hat{G}_{27}$ @ NNLO:

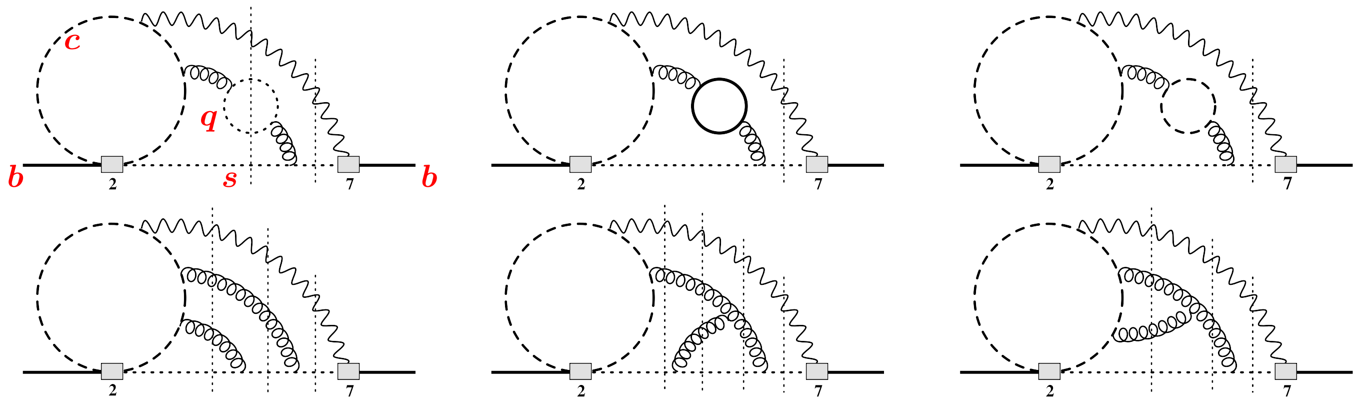

1. Generation of diagrams and performing the Dirac algebra to express everything in terms of (a few) $\times 10^5$ four-loop two-scale scalar integrals with unitarity cuts ($\mathcal{O}(500)$ families).

2. Reduction to master integrals (MIs) with the help of Integration By Parts (IBP) [KIRA]. $\mathcal{O}(1\,\mathrm{TB})$ RAM and weeks of CPU needed for the most complicated families.

3. Extending the set of master integrals M_k so that it closes under differentiation with respect to $z = m_c^2/m_b^2$. This way one obtains a system of differential equations

$$\frac{d}{dz} M_k(z,\epsilon) = \sum_l R_{kl}(z,\epsilon)\, M_l(z,\epsilon), \qquad (*)$$

where R_{nk} are rational functions of their arguments.

Sample diagrams contributing to $\hat{G}_{27}$ @ NNLO:

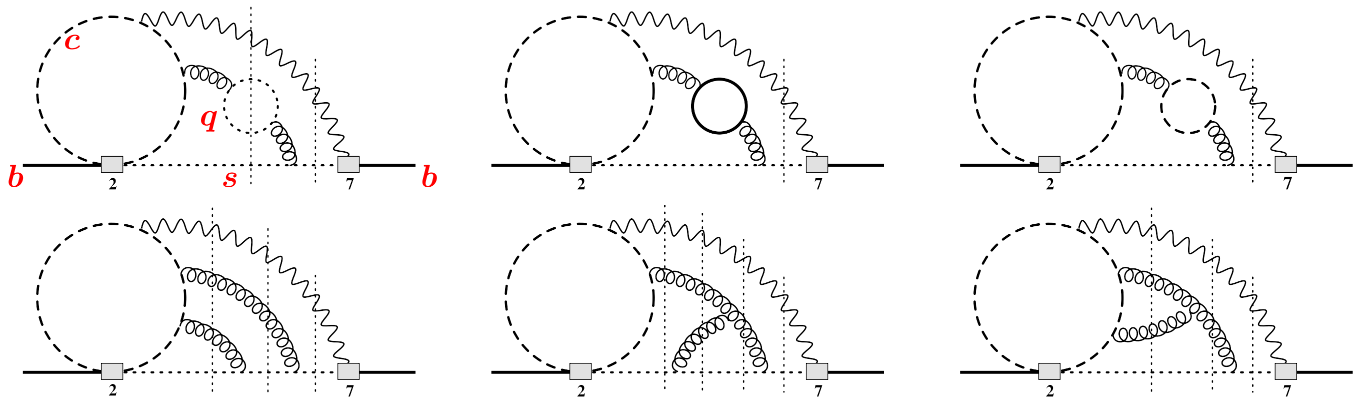

1. Generation of diagrams and performing the Dirac algebra to express everything in terms of (a few) $\times 10^5$ four-loop two-scale scalar integrals with unitarity cuts ($\mathcal{O}(500)$ families).

2. Reduction to master integrals (MIs) with the help of Integration By Parts (IBP) [KIRA]. $\mathcal{O}(1\,\mathrm{TB})$ RAM and weeks of CPU needed for the most complicated families.

3. Extending the set of master integrals M_k so that it closes under differentiation with respect to $z = m_c^2/m_b^2$. This way one obtains a system of differential equations

$$\frac{d}{dz} M_k(z,\epsilon) = \sum_l R_{kl}(z,\epsilon)\, M_l(z,\epsilon), \qquad (*)$$

where R_{nk} are rational functions of their arguments.

4. Calculating boundary conditions for $(*)$ using automatized asymptotic expansions at $m_c \gg m_b$.

Sample diagrams contributing to $\hat{G}_{27}$ @ NNLO:

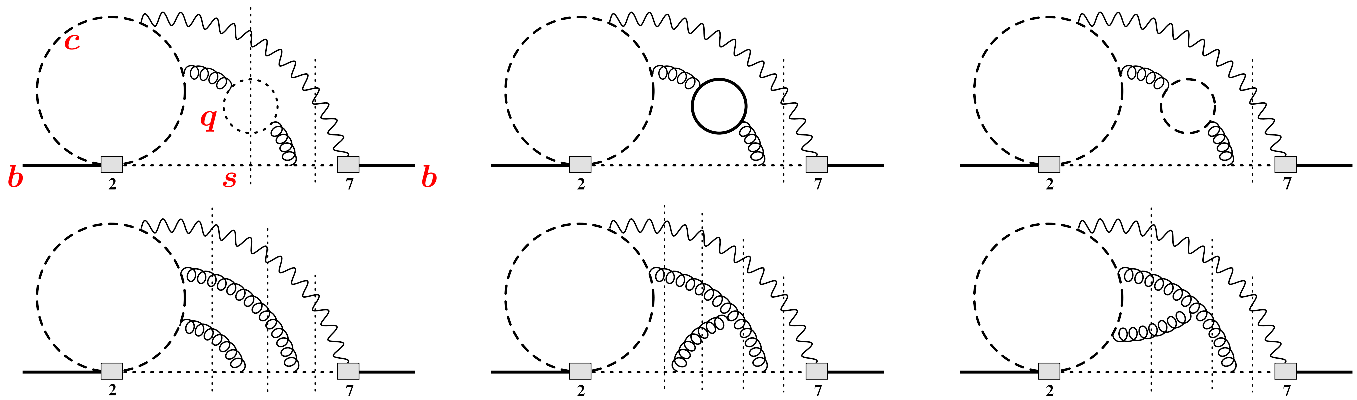

1. Generation of diagrams and performing the Dirac algebra to express everything in terms of (a few) $\times 10^5$ four-loop two-scale scalar integrals with unitarity cuts ($\mathcal{O}(500)$ families).

2. Reduction to master integrals (MIs) with the help of Integration By Parts (IBP) [KIRA]. $\mathcal{O}(1\,\mathrm{TB})$ RAM and weeks of CPU needed for the most complicated families.

3. Extending the set of master integrals M_k so that it closes under differentiation with respect to $z = m_c^2/m_b^2$. This way one obtains a system of differential equations

$$\frac{d}{dz} M_k(z,\epsilon) = \sum_l R_{kl}(z,\epsilon)\, M_l(z,\epsilon), \qquad (*)$$

where R_{nk} are rational functions of their arguments.

4. Calculating boundary conditions for $(*)$ using automatized asymptotic expansions at $m_c \gg m_b$.

5. Calculating three-loop single-scale master integrals for the boundary conditions.

Sample diagrams contributing to $\hat{G}_{27}$ @ NNLO:

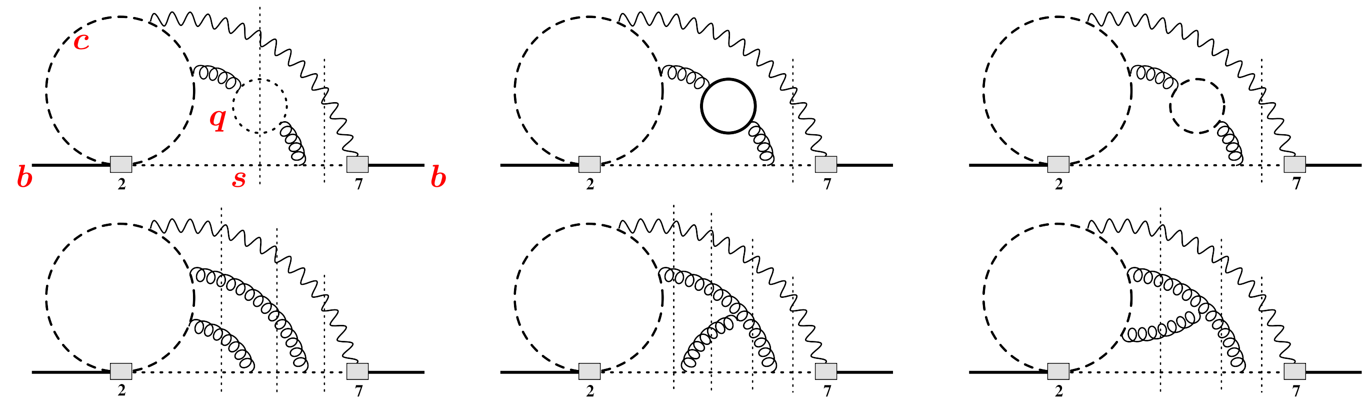

1. Generation of diagrams and performing the Dirac algebra to express everything in terms of (a few) $\times 10^5$ four-loop two-scale scalar integrals with unitarity cuts ($\mathcal{O}(500)$ families).

2. Reduction to master integrals (MIs) with the help of Integration By Parts (IBP) [KIRA]. $\mathcal{O}(1\,\text{TB})$ RAM and weeks of CPU needed for the most complicated families.

3. Extending the set of master integrals M_k so that it closes under differentiation with respect to $z = m_c^2/m_b^2$. This way one obtains a system of differential equations

$$\frac{d}{dz} M_k(z,\epsilon) = \sum_l R_{kl}(z,\epsilon)\, M_l(z,\epsilon), \qquad (*)$$

where R_{nk} are rational functions of their arguments.

4. Calculating boundary conditions for $(*)$ using automatized asymptotic expansions at $m_c \gg m_b$.

5. Calculating three-loop single-scale master integrals for the boundary conditions.

6. Solving the system $(*)$ numerically [A.C. Hindmarsch, http://www.netlib.org/odepack] along an ellipse in the complex z plane. Doing so along several different ellipses allows us to estimate the numerical error.

Another approach to bare 2-body contributions in arXiv:2309.14707

[M. Czaja, M. Czakon, T. Huber, M. Misiak, M. Niggetiedt, A. Rehman, K. Schönwald, M. Steinhauser]

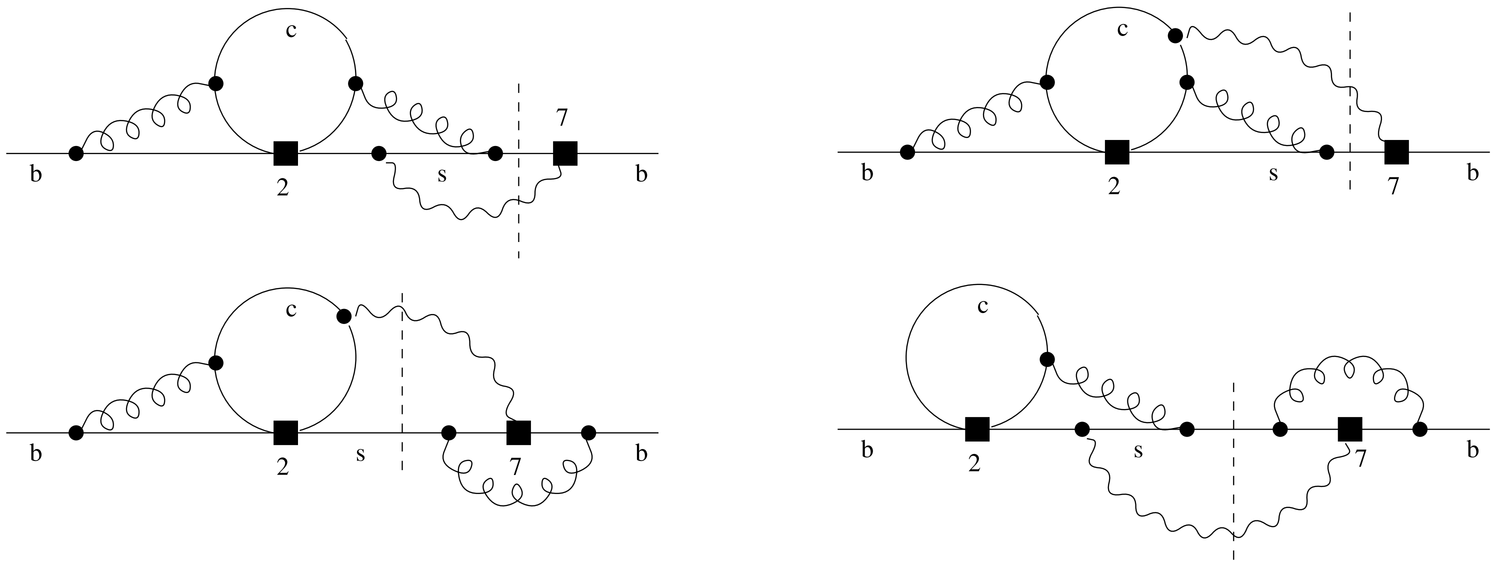

Another approach to bare 2-body contributions in arXiv:2309.14707

[M. Czaja, M. Czakon, T. Huber, M. Misiak, M. Niggetiedt, A. Rehman, K. Schönwald, M. Steinhauser]

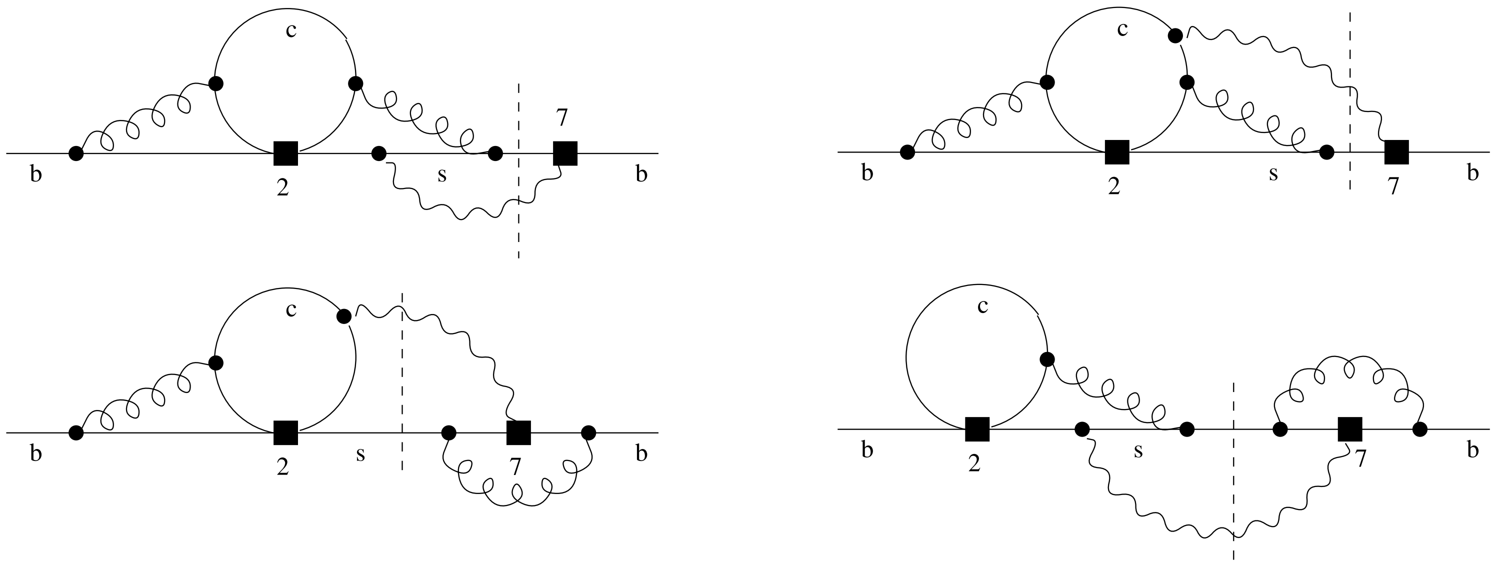

1. **The MIs are numerically calculated at the physical value of m_c using `AMFlow` [arXiv:2201.11669].**

Another approach to bare 2-body contributions in arXiv:2309.14707

[M. Czaja, M. Czakon, T. Huber, M. Misiak, M. Niggetiedt, A. Rehman, K. Schönwald, M. Steinhauser]

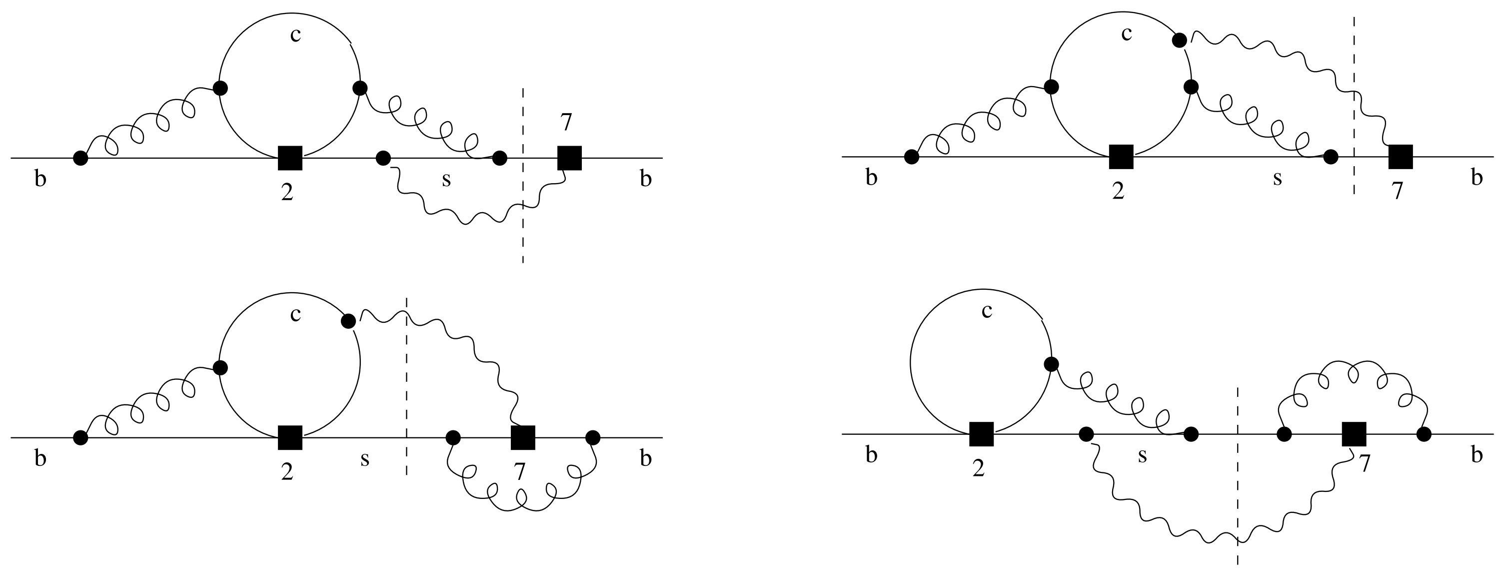

1. **The MIs are numerically calculated at the physical value of m_c using** `AMFlow` **[arXiv:2201.11669].**
2. **Thus, no expansions in the limit $m_c \gg m_b$ need to be determined. We have tested them though.**

Another approach to bare 2-body contributions in arXiv:2309.14707

[M. Czaja, M. Czakon, T. Huber, M. Misiak, M. Niggetiedt, A. Rehman, K. Schönwald, M. Steinhauser]

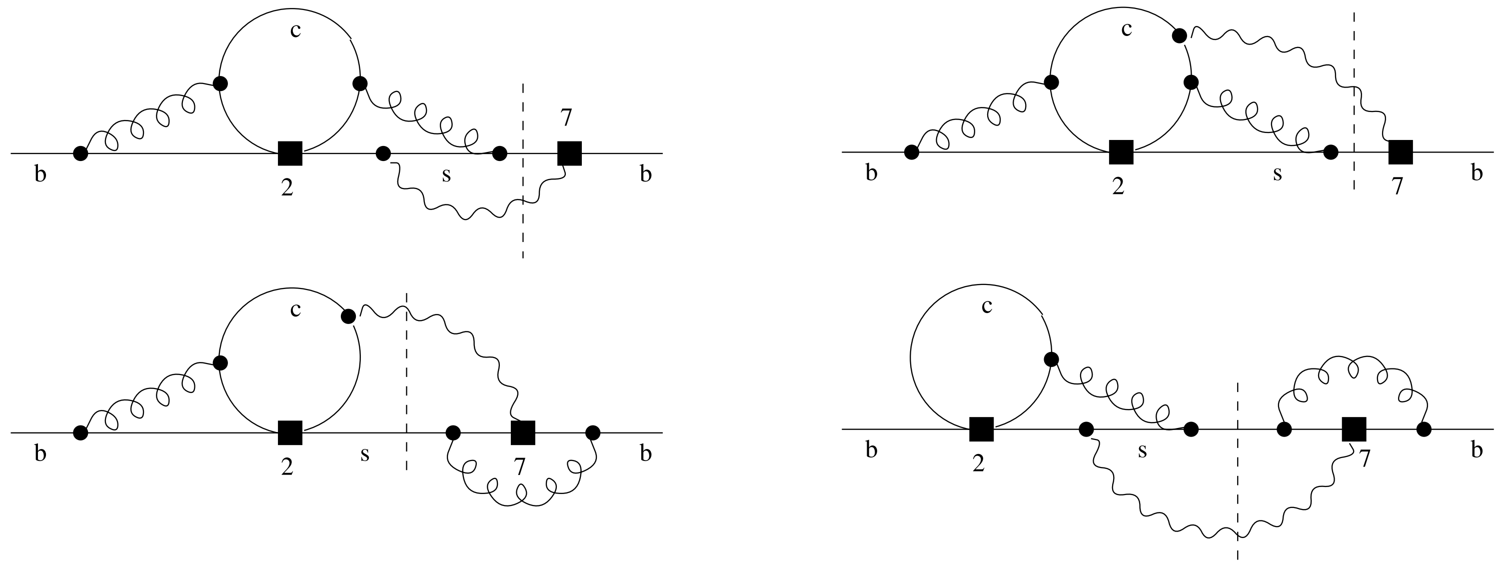

1. The MIs are numerically calculated at the physical value of m_c using `AMFlow` [arXiv:2201.11669].
2. Thus, no expansions in the limit $m_c \gg m_b$ need to be determined. We have tested them though.
3. UV and IR divergences are dimensionally regulated. The 2-body contributions alone are not IR safe.

Another approach to bare 2-body contributions in arXiv:2309.14707

[M. Czaja, M. Czakon, T. Huber, M. Misiak, M. Niggetiedt, A. Rehman, K. Schönwald, M. Steinhauser]

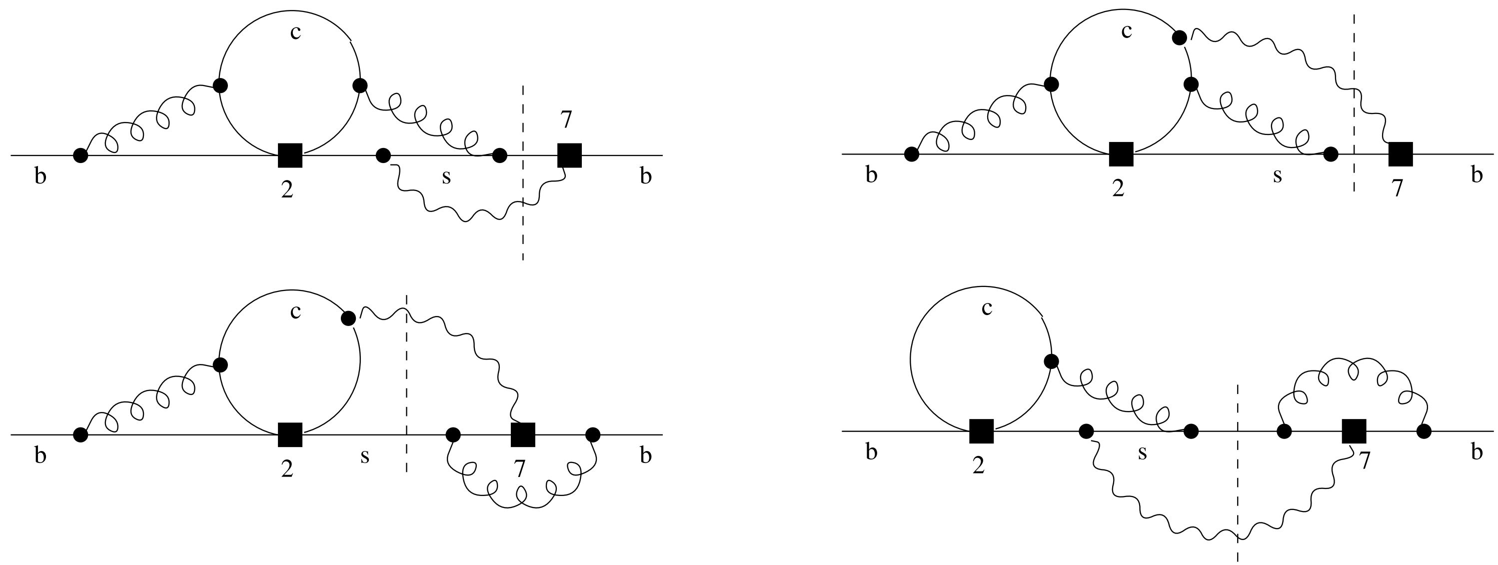

1. The MIs are numerically calculated at the physical value of m_c using `AMFlow` [arXiv:2201.11669].
2. Thus, no expansions in the limit $m_c \gg m_b$ need to be determined. We have tested them though.
3. UV and IR divergences are dimensionally regulated. The 2-body contributions alone are not IR safe.
4. Sample result: $\Delta_{21}\hat{G}_{27}^{(2)2P}(z) = \frac{368}{243\epsilon^3} + \frac{736-324f_0(z)}{243\epsilon^2} + \frac{1}{\epsilon}\left(\frac{1472}{243} + \frac{92}{729}\pi^2 - \frac{8f_0(z)+4f_1(z)}{3}\right) + p(z),$

Another approach to bare 2-body contributions in arXiv:2309.14707

[M. Czaja, M. Czakon, T. Huber, M. Misiak, M. Niggetiedt, A. Rehman, K. Schönwald, M. Steinhauser]

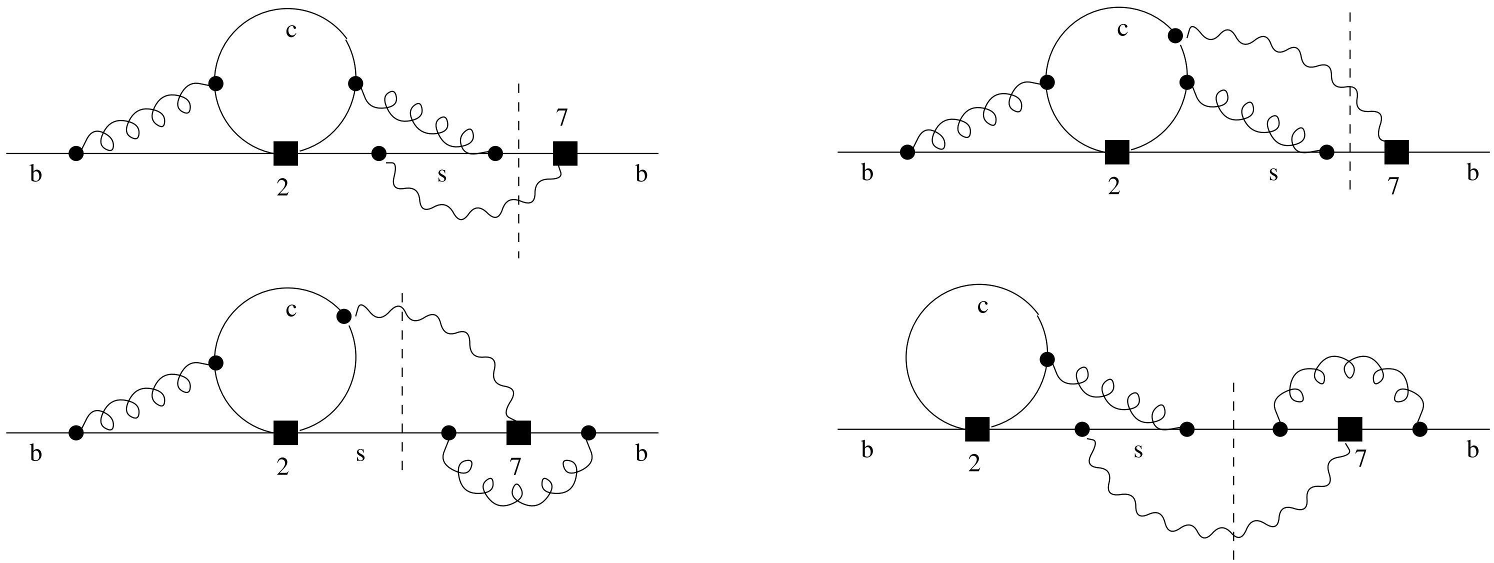

1. The MIs are numerically calculated at the physical value of m_c using `AMFlow` [arXiv:2201.11669].
2. Thus, no expansions in the limit $m_c \gg m_b$ need to be determined. We have tested them though.
3. UV and IR divergences are dimensionally regulated. The 2-body contributions alone are not IR safe.
4. Sample result: $\Delta_{21}\hat{G}_{27}^{(2)2P}(z) = \frac{368}{243\epsilon^3} + \frac{736-324f_0(z)}{243\epsilon^2} + \frac{1}{\epsilon}\left(\frac{1472}{243} + \frac{92}{729}\pi^2 - \frac{8f_0(z)+4f_1(z)}{3}\right) + p(z),$

   where $p(z=0.04) \simeq 144.959811.$

Another approach to bare 2-body contributions in arXiv:2309.14707

[M. Czaja, M. Czakon, T. Huber, M. Misiak, M. Niggetiedt, A. Rehman, K. Schönwald, M. Steinhauser]

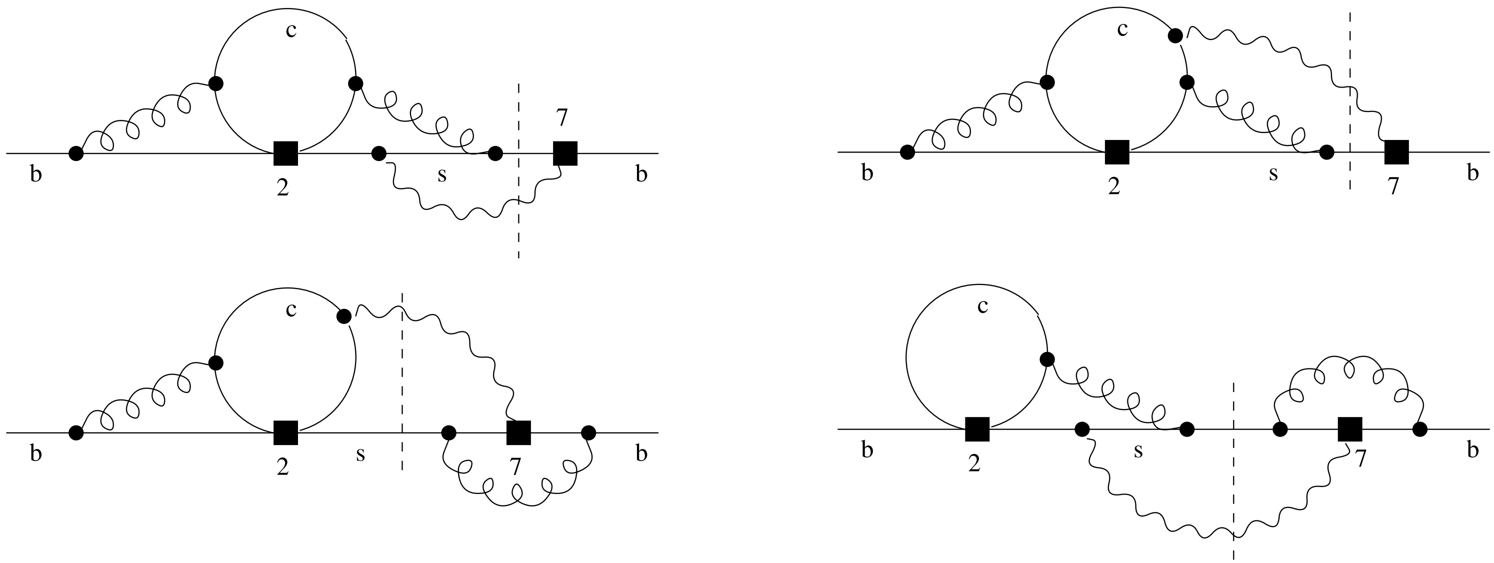

1. The MIs are numerically calculated at the physical value of m_c using `AMFlow` [arXiv:2201.11669].
2. Thus, no expansions in the limit $m_c \gg m_b$ need to be determined. We have tested them though.
3. UV and IR divergences are dimensionally regulated. The 2-body contributions alone are not IR safe.
4. Sample result: $\Delta_{21}\hat{G}_{27}^{(2)2P}(z) = \frac{368}{243\epsilon^3} + \frac{736-324f_0(z)}{243\epsilon^2} + \frac{1}{\epsilon}\left(\frac{1472}{243} + \frac{92}{729}\pi^2 - \frac{8f_0(z)+4f_1(z)}{3}\right) + p(z)$,

where $p(z=0.04) \simeq 144.959811$.

The large-z expansion of $p(z)$ reads:

$$p(z) = \tfrac{138530}{6561} - \tfrac{3680}{729}\zeta(3) - \tfrac{6136}{243}L + \tfrac{5744}{729}L^2 - \tfrac{1808}{729}L^3 + \tfrac{1}{z}\left(-\tfrac{4222952}{1366875} - \tfrac{602852}{273375}L + \tfrac{34568}{18225}L^2 - \tfrac{532}{1215}L^3\right)$$
$$+ \tfrac{1}{z^2}\left(-\tfrac{33395725469}{26254935000} - \tfrac{111861263}{93767625}L + \tfrac{156358}{178605}L^2 - \tfrac{172}{1215}L^3\right) + \mathcal{O}\left(\tfrac{1}{z^3}\right), \quad \text{with } L = \log z.$$

2-body contributions from vertex diagrams

in arXiv:2303.01714 [C. Greub, H.M. Asatrian, F. Saturnino, C. Wiegand]

and arXiv:2309.14706 [M. Fael, F. Lange, K. Schönwald, M. Steinhauser]

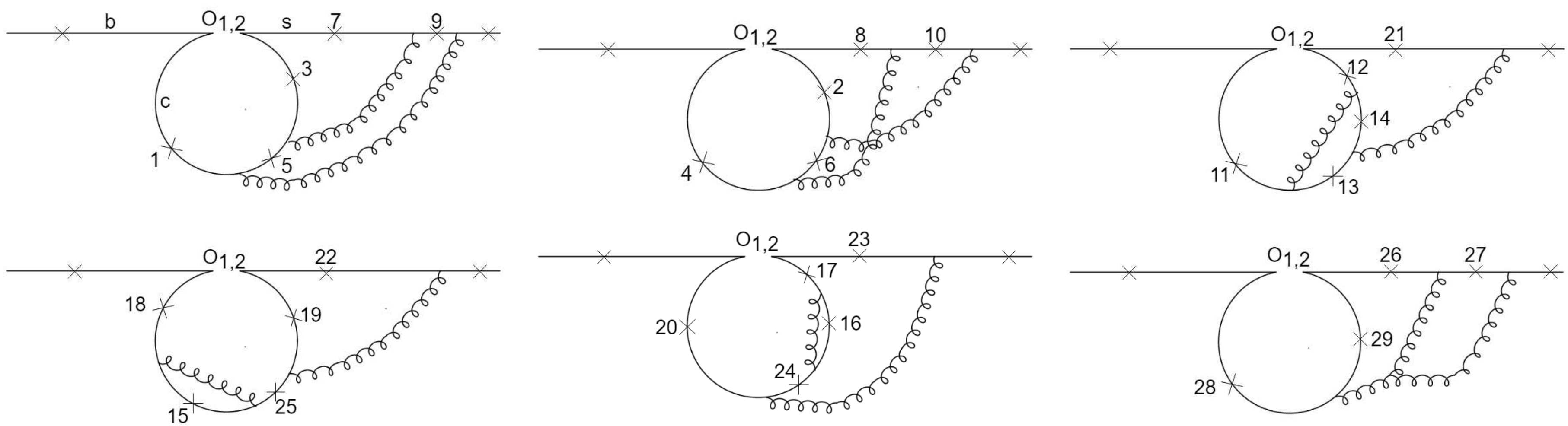

2-body contributions from vertex diagrams

in arXiv:2303.01714 [C. Greub, H.M. Asatrian, F. Saturnino, C. Wiegand]

and arXiv:2309.14706 [M. Fael, F. Lange, K. Schönwald, M. Steinhauser]

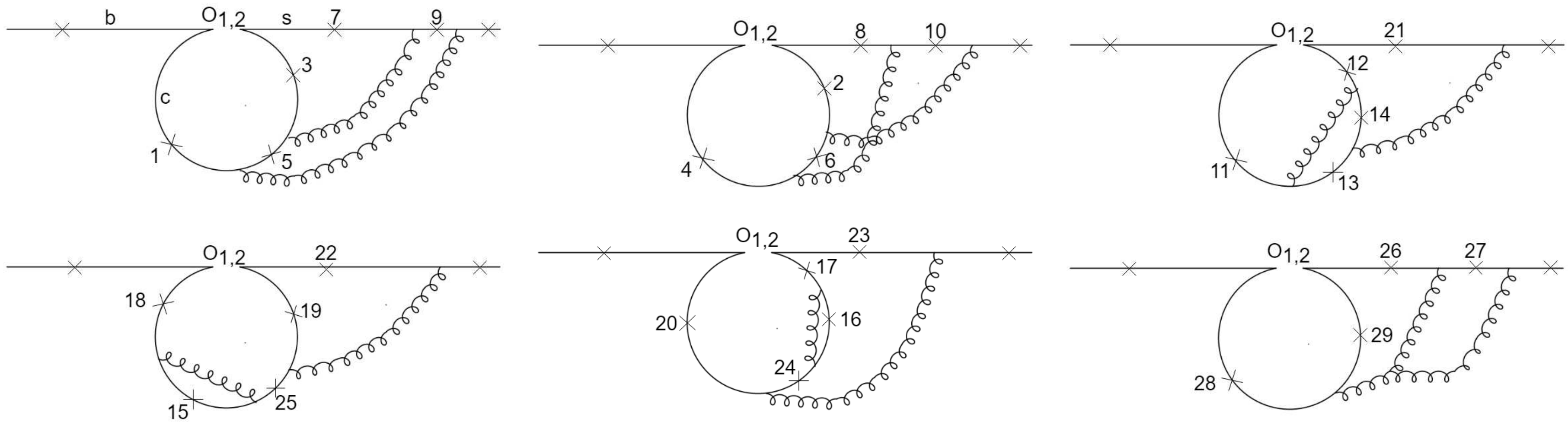

1. Amplitudes rather than interference terms.

2-body contributions from vertex diagrams

in arXiv:2303.01714 [C. Greub, H.M. Asatrian, F. Saturnino, C. Wiegand]

and arXiv:2309.14706 [M. Fael, F. Lange, K. Schönwald, M. Steinhauser]

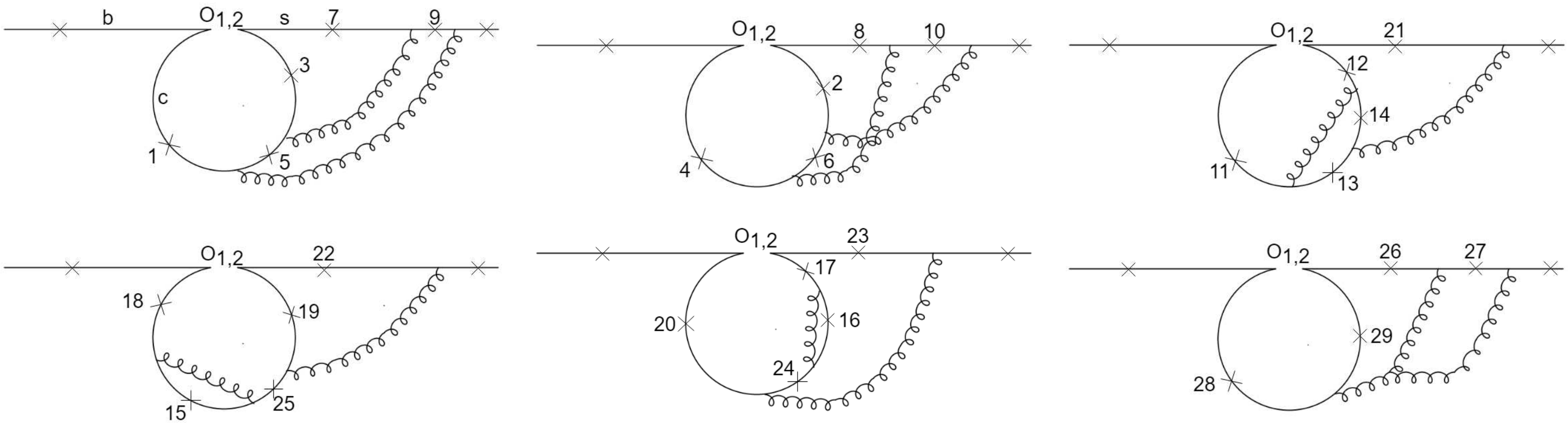

1. **Amplitudes rather than interference terms.**
2. **In arXiv:2303.01714: only diagrams with no gluon-(b-quark) couplings.**

2-body contributions from vertex diagrams

in arXiv:2303.01714 [C. Greub, H.M. Asatrian, F. Saturnino, C. Wiegand]

and arXiv:2309.14706 [M. Fael, F. Lange, K. Schönwald, M. Steinhauser]

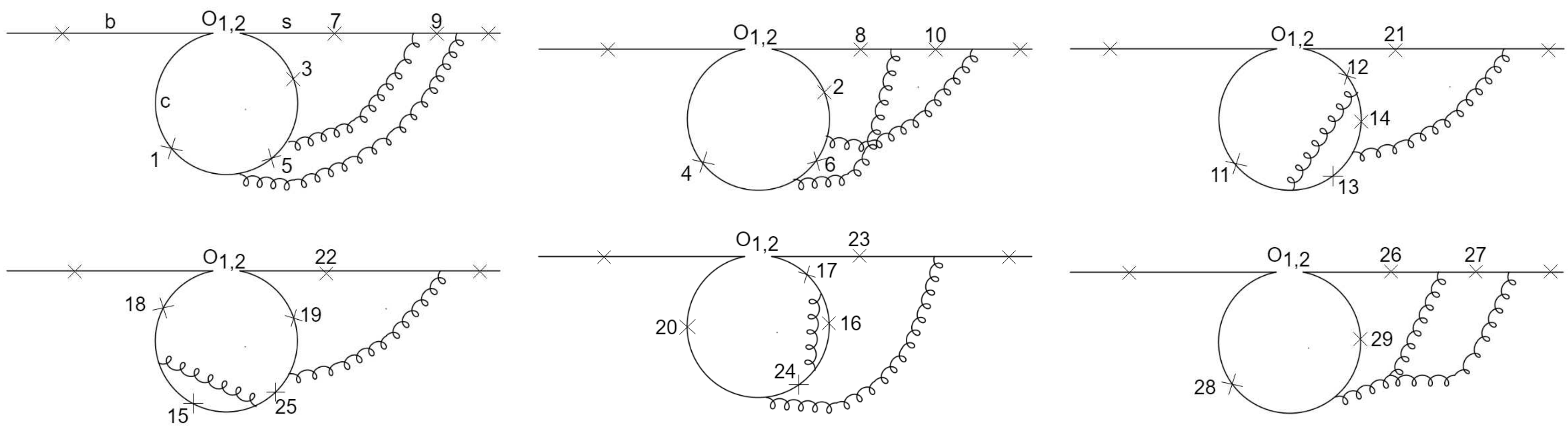

1. Amplitudes rather than interference terms.
2. In arXiv:2303.01714: only diagrams with no gluon-(b-quark) couplings.
3. IBP as usual. Then either `AMFlow` or differential equations starting from $m_c \gg m_b$.

2-body contributions from vertex diagrams

in arXiv:2303.01714 [C. Greub, H.M. Asatrian, F. Saturnino, C. Wiegand]

and arXiv:2309.14706 [M. Fael, F. Lange, K. Schönwald, M. Steinhauser]

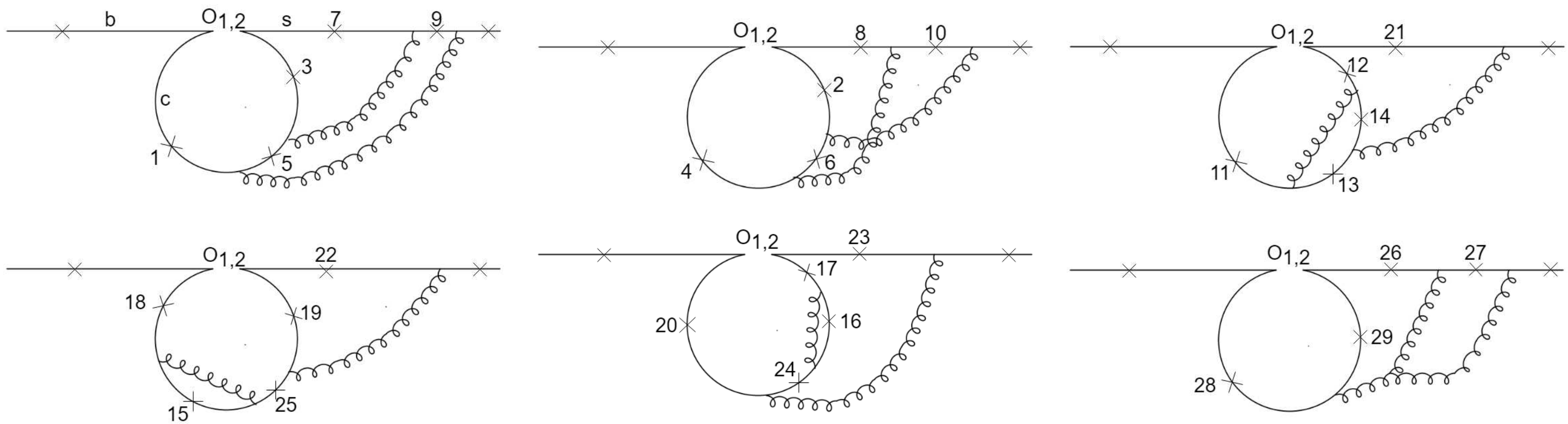

1. Amplitudes rather than interference terms.
2. In arXiv:2303.01714: only diagrams with no gluon-(b-quark) couplings.
3. IBP as usual. Then either `AMFlow` or differential equations starting from $m_c \gg m_b$.
4. Simplifying the differential equations and solving them analytically in many cases.

2-body contributions from vertex diagrams

in arXiv:2303.01714 [C. Greub, H.M. Asatrian, F. Saturnino, C. Wiegand]

and arXiv:2309.14706 [M. Fael, F. Lange, K. Schönwald, M. Steinhauser]

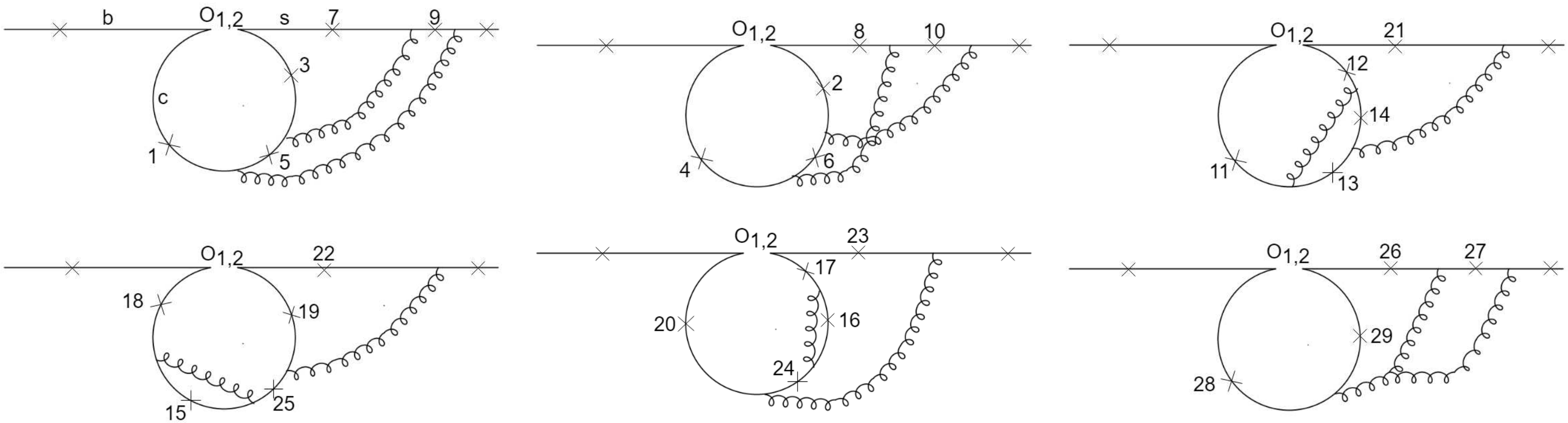

1. Amplitudes rather than interference terms.
2. In arXiv:2303.01714: only diagrams with no gluon-(b-quark) couplings.
3. IBP as usual. Then either `AMFlow` or differential equations starting from $m_c \gg m_b$.
4. Simplifying the differential equations and solving them analytically in many cases.
5. Fully analytical solutions at the two-loop level in arXiv:2309.14706.

Resolved photon contribution to the Q_7-$Q_{1,2}$ interference.

M.B. Voloshin, hep-ph/9612483; A. Khodjamirian, R. Rückl, G. Stoll and D. Wyler, hep-ph/9702318; Z. Ligeti, L. Randall and M.B. Wise, hep-ph/9702322; G. Buchalla, G. Isidori, G. Rey, hep-ph/9705253; M. Benzke, S.J. Lee, M. Neubert, G. Paz, arXiv:1003.5012; A. Gunawardana, G. Paz, arXiv:1908.02812.

$\langle \bar{B} |$ 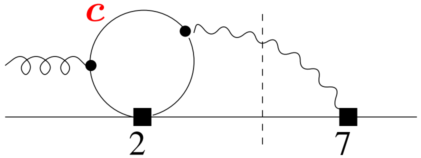 $| \bar{B} \rangle$

$$\delta N(E_0) = \left(C_2 - \tfrac{1}{6} C_1\right) C_7 \underbrace{\left[-\frac{\mu_G^2}{27 m_c^2} + \frac{\Lambda_{17}}{m_b} \right]}_{-\frac{\kappa_V \mu_G^2}{27 m_c^2}}$$

Resolved photon contribution to the Q_7-$Q_{1,2}$ interference.

M.B. Voloshin, hep-ph/9612483; A. Khodjamirian, R. Rückl, G. Stoll and D. Wyler, hep-ph/9702318;
Z. Ligeti, L. Randall and M.B. Wise, hep-ph/9702322; G. Buchalla, G. Isidori, G. Rey, hep-ph/9705253;
M. Benzke, S.J. Lee, M. Neubert, G. Paz, arXiv:1003.5012; A. Gunawardana, G. Paz, arXiv:1908.02812.

$\langle \bar{B} |$ 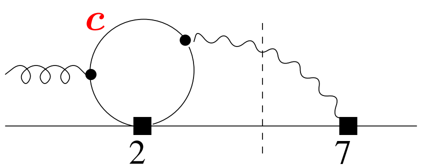 $| \bar{B} \rangle$

$$\delta \mathrm{N}(\mathrm{E}_0) = \left(C_2 - \tfrac{1}{6} C_1\right) C_7 \underbrace{\left[-\frac{\mu_{\mathrm{G}}^2}{27 \mathrm{m}_{\mathrm{c}}^2} + \frac{\Lambda_{17}}{\mathrm{m_b}} \right]}_{-\frac{\kappa_{\mathrm{V}} \mu_G^2}{27 m_c^2}}$$

$$\Lambda_{17} = \tfrac{2}{3} \mathrm{Re} \int_{-\infty}^{\infty} \frac{d\omega_1}{\omega_1} \left[1 - F\left(\frac{m_c^2 - i\varepsilon}{m_b \omega_1} \right) + \frac{m_b \omega_1}{12 m_c^2} \right] h_{17}(\omega_1, \mu)$$

$\omega_1 \leftrightarrow$ gluon momentum, $\quad F(x) = 4x \arctan^2 \left(1/\sqrt{4x-1}\right)$

Resolved photon contribution to the Q_7-$Q_{1,2}$ interference.

M.B. Voloshin, hep-ph/9612483; A. Khodjamirian, R. Rückl, G. Stoll and D. Wyler, hep-ph/9702318;
Z. Ligeti, L. Randall and M.B. Wise, hep-ph/9702322; G. Buchalla, G. Isidori, G. Rey, hep-ph/9705253;
M. Benzke, S.J. Lee, M. Neubert, G. Paz, arXiv:1003.5012; A. Gunawardana, G. Paz, arXiv:1908.02812.

$\langle \bar{B}|$ 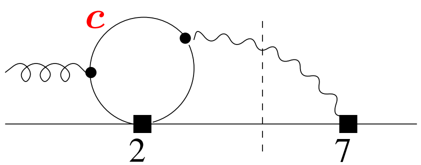 $|\bar{B}\rangle$

$$\delta N(E_0) = (C_2 - \tfrac{1}{6}C_1)C_7 \underbrace{\left[-\frac{\mu_G^2}{27m_c^2} + \frac{\Lambda_{17}}{m_b} \right]}_{-\frac{\kappa_V \mu_G^2}{27m_c^2}}$$

$$\Lambda_{17} = \tfrac{2}{3}\mathrm{Re}\int_{-\infty}^{\infty} \frac{d\omega_1}{\omega_1}\left[1 - F\left(\frac{m_c^2 - i\varepsilon}{m_b\omega_1}\right) + \frac{m_b\omega_1}{12m_c^2}\right] h_{17}(\omega_1,\mu)$$

$\omega_1 \leftrightarrow$ gluon momentum, $\qquad F(x) = 4x\arctan^2\left(1/\sqrt{4x-1}\right)$

The soft function h_{17}:

$$h_{17}(\omega_1,\mu) = \int \frac{dr}{4\pi M_B} e^{-i\omega_1 r}\langle \bar{B}|(\bar{h}S_{\bar{n}})(0)\not{\bar{n}}\, i\gamma_\alpha^\perp \bar{n}_\beta (S_{\bar{n}}^\dagger g G_s^{\alpha\beta} S_{\bar{n}})(r\bar{n})(S_{\bar{n}}^\dagger h)(0)|\bar{B}\rangle \qquad (m_b - 2E_0 \gg \Lambda_{\rm QCD})$$

A class of models for h_{17}: $\qquad h_{17}(\omega_1,\mu) = e^{-\frac{\omega_1^2}{2\sigma^2}} \sum_n a_{2n} H_{2n}\left(\frac{\omega_1}{\sigma\sqrt{2}}\right), \qquad \sigma < 1$ GeV

Hermite polynomials

Constraints on moments (e.g.): $\quad \int d\omega_1 h_{17} = \frac{2}{3}\mu_G^2, \qquad \int d\omega_1 \omega_1^2 h_{17} = \frac{2}{15}(5m_5 + 3m_6 - 2m_9).$

Resolved photon contribution to the Q_7-$Q_{1,2}$ interference.

M.B. Voloshin, hep-ph/9612483; A. Khodjamirian, R. Rückl, G. Stoll and D. Wyler, hep-ph/9702318;
Z. Ligeti, L. Randall and M.B. Wise, hep-ph/9702322; G. Buchalla, G. Isidori, G. Rey, hep-ph/9705253;
M. Benzke, S.J. Lee, M. Neubert, G. Paz, arXiv:1003.5012; A. Gunawardana, G. Paz, arXiv:1908.02812.

$\langle \bar{B}|$ 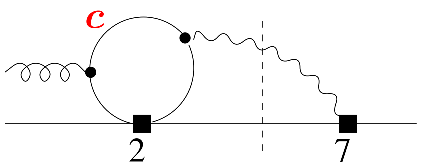 $|\bar{B}\rangle$

$$\delta \mathrm{N(E_0)} = (C_2 - \tfrac{1}{6}C_1)C_7 \underbrace{\left[-\frac{\mu_G^2}{27 m_c^2} + \frac{\Lambda_{17}}{m_b} \right]}_{-\frac{\kappa_V \mu_G^2}{27 m_c^2}}$$

$$\Lambda_{17} = \tfrac{2}{3}\mathrm{Re}\int_{-\infty}^{\infty} \frac{d\omega_1}{\omega_1} \left[1 - F\left(\frac{m_c^2 - i\varepsilon}{m_b \omega_1}\right) + \frac{m_b \omega_1}{12 m_c^2} \right] h_{17}(\omega_1, \mu)$$

$\omega_1 \leftrightarrow$ gluon momentum, $\qquad F(x) = 4x \arctan^2\left(1/\sqrt{4x-1}\right)$

The soft function h_{17}:

$$h_{17}(\omega_1, \mu) = \int \frac{dr}{4\pi M_B} e^{-i\omega_1 r} \langle \bar{B}|(\bar{h} S_{\bar{n}})(0) \not{\bar{n}}\, i\gamma_\alpha^\perp \bar{n}_\beta (S_{\bar{n}}^\dagger g G_s^{\alpha\beta} S_{\bar{n}})(r\bar{n})(S_{\bar{n}}^\dagger h)(0)|\bar{B}\rangle \qquad (m_b - 2E_0 \gg \Lambda_{\rm QCD})$$

A class of models for h_{17}: $\qquad h_{17}(\omega_1, \mu) = e^{-\frac{\omega_1^2}{2\sigma^2}} \sum_n a_{2n} H_{2n}\left(\frac{\omega_1}{\sigma\sqrt{2}}\right), \qquad \sigma < 1$ GeV

Hermite polynomials

Constraints on moments (e.g.): $\quad \int d\omega_1 h_{17} = \frac{2}{3}\mu_G^2, \qquad \int d\omega_1 \omega_1^2 h_{17} = \frac{2}{15}(5m_5 + 3m_6 - 2m_9).$

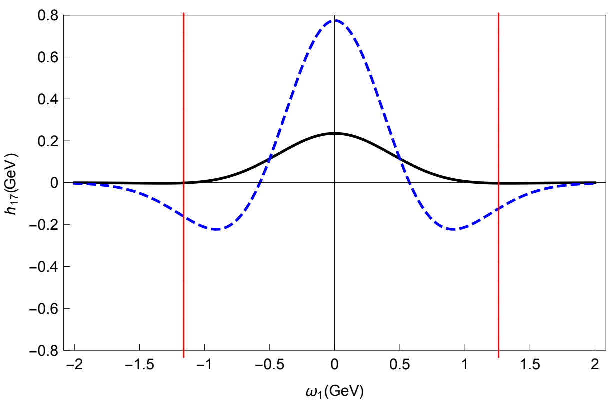

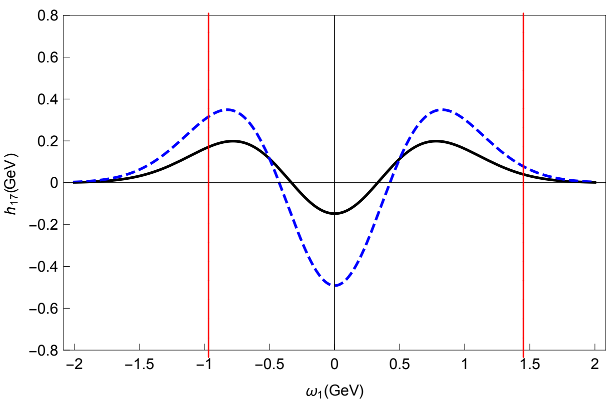

Resolved photon contribution to the Q_7-$Q_{1,2}$ interference.

M.B. Voloshin, hep-ph/9612483; A. Khodjamirian, R. Rückl, G. Stoll and D. Wyler, hep-ph/9702318;
Z. Ligeti, L. Randall and M.B. Wise, hep-ph/9702322; G. Buchalla, G. Isidori, G. Rey, hep-ph/9705253;
M. Benzke, S.J. Lee, M. Neubert, G. Paz, arXiv:1003.5012; A. Gunawardana, G. Paz, arXiv:1908.02812.

$\langle \bar{B} |$ 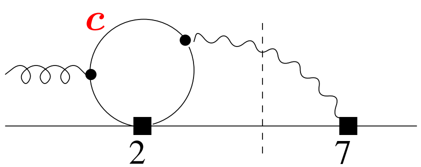 $| \bar{B} \rangle$

$$\delta \mathrm{N}(\mathrm{E}_0) = (C_2 - \tfrac{1}{6} C_1) C_7 \underbrace{\left[-\frac{\mu_G^2}{27 m_c^2} + \frac{\Lambda_{17}}{m_b} \right]}_{-\frac{\kappa_V \mu_G^2}{27 m_c^2}}$$

$$\Lambda_{17} = \tfrac{2}{3} \mathrm{Re} \int_{-\infty}^{\infty} \frac{d\omega_1}{\omega_1} \left[1 - F\left(\frac{m_c^2 - i\varepsilon}{m_b \omega_1} \right) + \frac{m_b \omega_1}{12 m_c^2} \right] h_{17}(\omega_1, \mu)$$

$\omega_1 \leftrightarrow$ gluon momentum, $\qquad F(x) = 4x \arctan^2 \left(1/\sqrt{4x-1} \right)$

The soft function h_{17}:

$$h_{17}(\omega_1, \mu) = \int \frac{dr}{4\pi M_B} e^{-i\omega_1 r} \langle \bar{B} | (\bar{h} S_{\bar{n}})(0) \not{\bar{n}}\, i \gamma_\alpha^\perp \bar{n}_\beta (S_{\bar{n}}^\dagger g G_s^{\alpha\beta} S_{\bar{n}})(r\bar{n}) (S_{\bar{n}}^\dagger h)(0) | \bar{B} \rangle \qquad (m_b - 2E_0 \gg \Lambda_{\mathrm{QCD}})$$

A class of models for h_{17}: $\qquad h_{17}(\omega_1, \mu) = e^{-\frac{\omega_1^2}{2\sigma^2}} \sum_n a_{2n} H_{2n} \left(\frac{\omega_1}{\sigma\sqrt{2}} \right), \qquad \sigma < 1$ GeV

Hermite polynomials

Constraints on moments (e.g.): $\quad \int d\omega_1 h_{17} = \frac{2}{3} \mu_G^2, \qquad \int d\omega_1 \omega_1^2 h_{17} = \frac{2}{15} (5 m_5 + 3 m_6 - 2 m_9).$

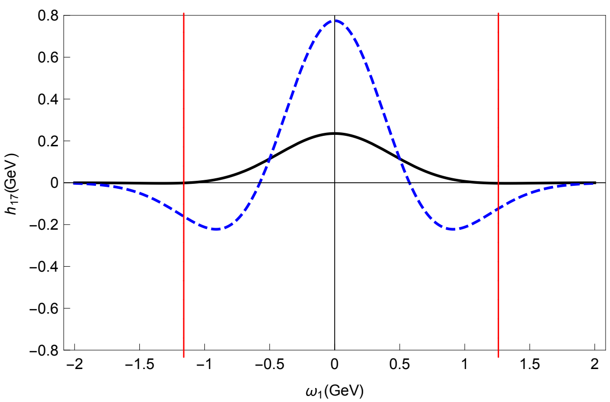

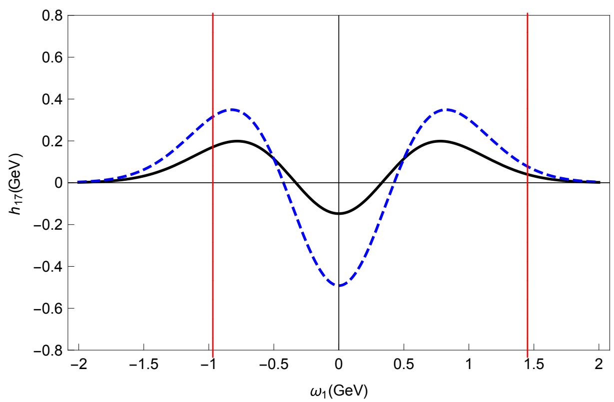

G+P numerically:
$\Lambda_{17} \in [-24, 5]$ MeV for $m_c = 1.17$ GeV.

Factor-of-3 improvement w.r.t. BLNP.

In our code: $\kappa_V = 1.2 \pm 0.3$.
Warning: scheme for m_c!

Moment constraints vs. models of h_{17}

M. Benzke, S.J. Lee, M. Neubert, G. Paz, arXiv:1003.5012 – only the leading moment included.

A. Gunawardana, G. Paz, arXiv:1908.02812 – estimates of the subleading moments from LLSA included.

M. Benzke, T. Hurth, arXiv:2006.00624 – as above but with more generous modeling and partial $1/m_b^2$ corrections.

Plots from the latter article:

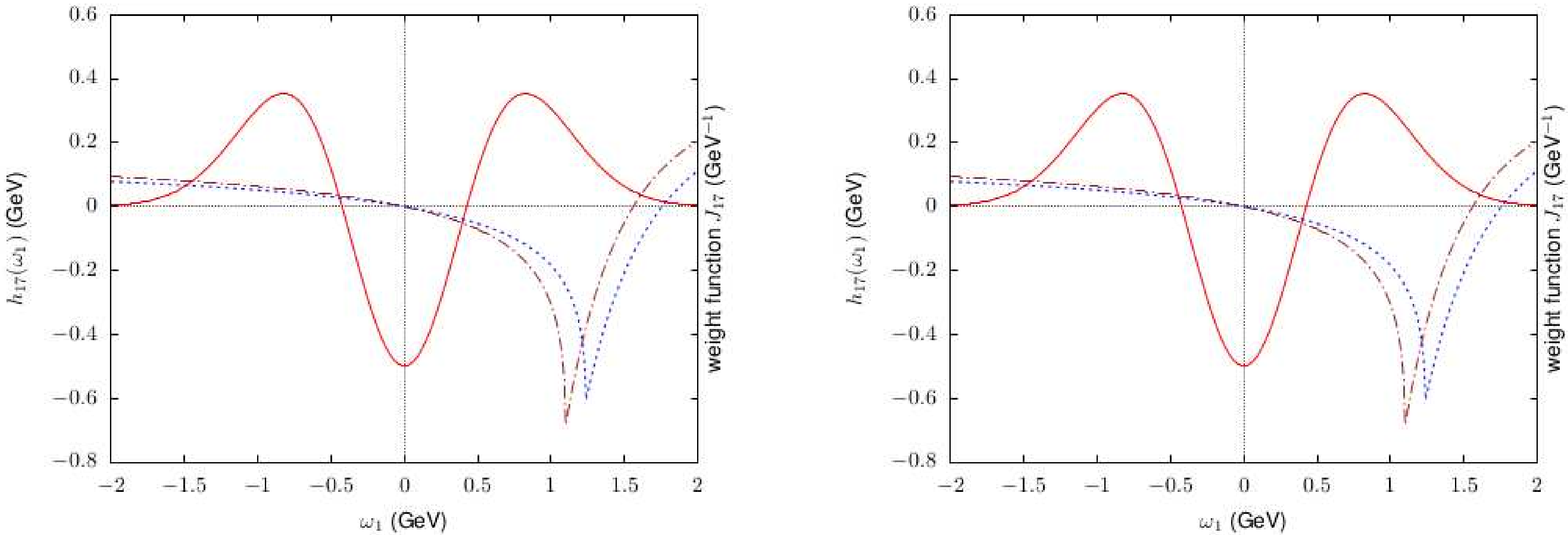

Another recent contribution: clarifying the SCET treatment of resolved photons in the Q_8-Q_8 interference; T. Hurth and R. Szafron, arXiv:2301.01739.

Inclusive determinations of $|V_{cb}|$ with $\mathcal{O}(\alpha_s^3)$ effects.

$$
\begin{aligned}
\Gamma(\bar{B} \to X_c e \bar{\nu}) &= \Gamma_0 f(\rho) \left[1 + a_1 \frac{\alpha_s}{\pi} + a_2 \left(\frac{\alpha_s}{\pi}\right)^2 + a_3 \left(\frac{\alpha_s}{\pi}\right)^3 \right. \\
&\quad \left. - \left(\frac{1}{2} - p_1 \frac{\alpha_s}{\pi}\right) \frac{\mu_\pi^2}{m_b^2} + \left(g_0 + g_1 \frac{\alpha_s}{\pi}\right) \frac{\mu_G^2}{m_b^2} + d_0 \frac{\rho_D^3}{m_b^3} - g_0 \frac{\rho_{LS}^3}{m_b^3} + \ldots \right]
\end{aligned}
\qquad (1)
$$

$$\Gamma_0 = \frac{G_F^2 m_{b,\text{kin}}^5 |V_{cb}|^2 A_{ew}}{192\pi^3}, \qquad f(\rho) = 1 - 8\rho + 8\rho^3 - \rho^4 - 12\rho^2 \ln \rho, \qquad \rho = \overline{m}_c^2(\mu_c)/m_{b,\text{kin}}^2.$$

1. Evaluation of a_3: M. Fael, K. Schönwald, M. Steinhauser, arXiv:2011.13654.

2. Finding $\dfrac{m_{b,\text{kin}}}{m_{b,\text{pole}}}$ up to $\mathcal{O}(\alpha_s^3)$: M. Fael, K. Schönwald, M. Steinhauser, arXiv:2005.06487, arXiv:2011.11655.

3. Lepton-energy moment fit including $\mathcal{O}(\alpha_s^3)$: M. Bordone, B. Capdevila, P. Gambino, arXiv:2107.00604.
   $\Rightarrow \quad |V_{cb}| = (42.16 \pm 0.51) \times 10^{-3}$

4. Evaluation of several $\overbrace{e\bar{\nu}\text{ invariant mass squared}}^{q^2}$ moments up to $\mathcal{O}(\alpha_s^3)$:
   M. Fael, K. Schönwald, M. Steinhauser, arXiv:2205.03410.

5. Extraction of $|V_{cb}|$ from q^2-moments:
   F. Bernlochner, M. Fael, K. Olschewsky, E. Persson, R. van Tonder, K. Vos, M. Welsch, arXiv:2205.10274.
   $\Rightarrow \quad |V_{cb}| = (41.69 \pm 0.63) \times 10^{-3}$

6. ...

Summary

- In the absence (?) of large NP effects in flavour physics, precision calculations are particularly relevant for the SM contributions.

- The measured $B_s \to \mu^+\mu^-$ and $\bar{B} \to X_s\gamma$ branching ratios agree within 1σ with the corresponding SM predictions.

- Further improvement of TH accuracy in $\bar{B} \to X_s\gamma$ requires getting rid of the interpolation in m_c at $\mathcal{O}(\alpha_s^2)$, as well as resolving the resolved photon issues.

- In the $B_s \to \mu^+\mu^-$ case, the main uncertainty comes from $|V_{cb}|$.

- Future determinations of $|V_{cb}|$ from q^2 moments will hopefully lead to further reduction of uncertainties.